

AD-A246 919



2

NAVAL POSTGRADUATE SCHOOL

Monterey, California



DTIC
ELECTE
MAR 05 1992
S D

THESIS

STUDIES IN CHAOS USING
STOCHASTIC METHODS

by
Edward A. Healy, JR

June, 1991

Thesis Advisor:

Ramesh Kolar

Approved for public release; distribution is unlimited

92-05683

UNCLASSIFIED

SECURITY CLASSIFICATION OF THIS PAGE

REPORT DOCUMENTATION PAGE				Form Approved OMB No. 0704-0188	
1a REPORT SECURITY CLASSIFICATION Unclassified			1b RESTRICTIVE MARKINGS		
2a SECURITY CLASSIFICATION AUTHORITY			3 DISTRIBUTION/AVAILABILITY OF REPORT Approved for public release; Distribution		
2b DECLASSIFICATION/DOWNGRADING SCHEDULE			5 MONITORING ORGANIZATION REPORT NUMBER(S)		
4. PERFORMING ORGANIZATION REPORT NUMBER(S)			5 MONITORING ORGANIZATION REPORT NUMBER(S)		
6a NAME OF PERFORMING ORGANIZATION Naval Postgraduate School		6b OFFICE SYMBOL (If applicable) 31	7a. NAME OF MONITORING ORGANIZATION Naval Postgraduate School		
6c. ADDRESS (City, State, and ZIP Code) Monterey, CA 93943-5000			7b ADDRESS (City, State, and ZIP Code) Monterey, CA 93943-5000		
8a NAME OF FUNDING/SPONSORING ORGANIZATION		8b OFFICE SYMBOL (If applicable)	9 PROCUREMENT INSTRUMENT IDENTIFICATION NUMBER		
8c. ADDRESS (City, State, and ZIP Code)			10 SOURCE OF FUNDING NUMBERS		
			PROGRAM ELEMENT NO	PROJECT NO	TASK NO
			WORK UNIT ACCESSION NO.		
11 TITLE (Include Security Classification) Studies in Chaos Using Stochastic Methods					
12 PERSONAL AUTHOR(S) Edward A. Healy, Jr.					
13a TYPE OF REPORT Master's Thesis		13b TIME COVERED FROM _____ TO _____		14 DATE OF REPORT (Year, Month, Day) June 1991	
				15 PAGE COUNT 82	
16 SUPPLEMENTARY NOTATION The views expressed in this thesis are those of the author and do not reflect the official policy or position of the Dept. of Defense of U.S. Government.					
17 COSATI CODES			18 SUBJECT TERMS (Continue on reverse if necessary and identify by block number)		
FIELD	GROUP	SUB-GROUP	chaos, Lorenz, duffing, fractal dimension, multivariate scaling analysis		
19 ABSTRACT (Continue on reverse if necessary and identify by block number)					
<p>Methods of chaos have been used to classify many heretofore inexplicable nonlinear dynamical systems in fields as diverse as ecology to engineering and economics to meteorology. This thesis presents the mathematical background needed to understand chaos as well as the engineering techniques used to study the nature of dynamical systems. Several dynamical systems are studied using two probabilistic measures of chaos, fractal correlation dimension and the multivariate scaling analysis. A new technique for developing a multivariate scaling analysis using a time embedding procedure is presented. The dynamical systems studied include the Lorenz equations, Duffing's equation and helicopter flight vibrations.</p>					
20 DISTRIBUTION/AVAILABILITY OF ABSTRACT <input checked="" type="checkbox"/> UNCLASSIFIED/UNLIMITED <input type="checkbox"/> SAME AS RPT <input type="checkbox"/> DTIC USERS			21 ABSTRACT SECURITY CLASSIFICATION Unclassified		
22a NAME OF RESPONSIBLE INDIVIDUAL Ramesh Kolar			22b TELEPHONE (Include Area Code) 408 646-2936		22c OFFICE SYMBOL AA/Kj

Approved for public release; distribution is unlimited.

Studies in Chaos using Stochastic Methods

by

Edward A. Healy, JR
Captain, United States Army
B.S., United States Military Academy, 1981

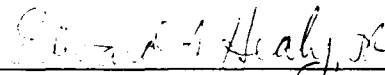
Submitted in partial fulfillment
of the requirements for the degree of

MASTER OF SCIENCE IN AERONAUTICAL ENGINEERING

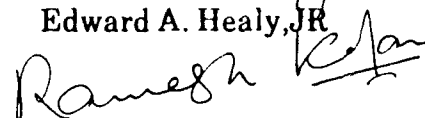
from the

NAVAL POSTGRADUATE SCHOOL
June 1991

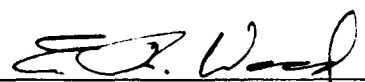
Author:


Edward A. Healy, JR

Approved by:


Ramesh Kolar, Thesis Advisor


Martinus Sarigul-Klijn, Second Reader


E. Roberts Wood, Chairman
Department of Aeronautics and Astronautics

ABSTRACT

Methods of chaos have been used to classify many heretofore inexplicable nonlinear dynamical systems in fields as diverse as ecology to engineering and economics to meteorology. This thesis presents the mathematical background needed to understand chaos as well as the engineering techniques used to study the nature of dynamical systems. Several dynamical systems are studied using two probabilistic measures of chaos, fractal correlation dimension and the multivariate scaling analysis. A new technique for developing a multivariate scaling analysis using a time embedding procedure is presented. The dynamical systems studied include the Lorenz equations, Duffing's equation and helicopter flight vibrations.

Accession For	
NTIS CRA&I	<input checked="" type="checkbox"/>
DTIC TAB	<input type="checkbox"/>
Unannounced	<input type="checkbox"/>
Justification	
By	
Distribution /	
Availability Codes	
Dist	Avail and for Special
A-1	

TABLE OF CONTENTS

I.	INTRODUCTION.....	1
A.	BACKGROUND.....	1
B.	OVERVIEW OF THESIS.....	3
II.	UNDERSTANDING CHAOS.....	5
A.	INTRODUCTION.....	5
B.	MATHEMATICAL BASIS FOR CHAOS.....	5
C.	ENGINEERING TECHNIQUES.....	14
1.	Time Domain Analysis.....	15
2.	Frequency Domain Analysis.....	15
3.	Phase Planes and Pseudo Phase Planes.....	16
4.	Van Der Pol Planes.....	18
5.	Lyapunov Exponents.....	19
6.	Fractal Dimension.....	20
7.	Evolving Measures of Chaos.....	20
D.	SUMMARY.....	21
E.	LITERATURE REVIEW.....	22
III.	METHODOLOGY.....	30
A.	INTRODUCTION.....	30
B.	SIMULATING A CONTINUOUS SYSTEM.....	30
C.	AN OVERVIEW OF SARIGUL-KLIJN'S WORK.....	33
D.	MULTIVARIATE SCALING ANALYSIS.....	35
E.	COMPUTER SIMULATIONS.....	37

IV. RESULTS.....	39
A. INTRODUCTION.....	39
B. RANDOM COLORED NOISE.....	39
C. LORENZ EQUATIONS.....	40
D. DUFFING'S EQUATIONS.....	42
E. HELICOPTER VIBRATION DATA.....	43
F. CONCLUSIONS.....	43
V. CONCLUSIONS AND SCOPE FOR FUTURE RESEARCH.....	62
APPENDIX A-PROGRAM TO PERFORM NUMERICAL INTEGRATION..	65
APPENDIX B-MULTIVARIATE SCALING ANALYSIS.....	68
LIST OF REFERENCES.....	72
INITIAL DISTRIBUTION LIST.....	75

I. INTRODUCTION

A. BACKGROUND

Mankind has used the ideas of science and mathematics to help understand, describe and control the world. The central notions of science have developed gradually. Truly revolutionary ideas do not often surface. The development of calculus by Newton and Leibnitz in the seventeenth century is quite possibly the last great revolutionary development in the sciences. Chaos and chaotic dynamics could very well be the next scientific revolution. The theories of chaotic dynamics are being used to describe and interpret many natural phenomenon that have heretofore been inexplicable.

The modern study of chaotic dynamical systems was begun by Henri Poincare at the beginning of the twentieth century. During his study of celestial bodies, Poincare observed that their trajectories were forever oscillating, yet irregular and aperiodic. Poincare described this motion as chaotic. He further discovered that the motion of a chaotic system has a very sensitive dependence on the initial conditions of the system. Because of the nonlinearity of chaotic systems, further rigorous study was impossible until the advent of the computer. Since 1960, many mathematicians and engineers have developed techniques to analyze chaotic systems. Much debate has occurred about the nature of chaos. Currently, the only

universally accepted property of chaotic dynamical systems is that they have sensitive dependence to initial conditions. Agreement about certain aspects of chaos does not exist within either the mathematical community or the engineering community and certainly no agreement exists between these groups.

In its David II report [Ref 1.1], the Committee on the Mathematical Sciences of the National Research Council, listed chaotic dynamics as one of the brightest areas for future advancement of applied mathematics. The report states that chaotic behavior has been found in nonlinear systems as diverse as ecology and economics to engineering and meteorology. The theories of chaos have their basis in the mathematical fields of topology, measure theory and combinatorics. Mathematicians are just now beginning to develop numerical methods for computing some of the properties which Poincare described some eighty years ago.

The engineering community looks at chaos from a different viewpoint. Engineers have developed techniques to analyze systems that have discrete data points to determine their chaotic tendencies. Pseudo phase planes, Lyapunov exponents and multivariate probability scaling analysis are but a few of the techniques that lend insight into the behavior of chaotic dynamical systems. No single method is completely conclusive. Hence, when studying nonlinear systems, a variety of methods is used.

The motivation for this thesis was twofold. First, an attempt has been made to bridge the gap between how mathematicians develop chaotic analysis and how engineers apply the methods of chaotic analysis. This was accomplished by examining systems that mathematicians have proven to be chaotic and using engineering methods to analyze these systems. The fortran program CHAOS developed by CDR Martinus Sarigul-Klijn [Ref. 1.2] while studying helicopter vibrations was used to analyze the Lorenz equations and Duffing's equation. Secondly, the data generated from the Lorenz equations, Duffing's equation and the helicopter vibration data used by CDR Sarigul-Klijn was analyzed using a new technique proposed by Osborne and Provenzale [Ref 1.3]. All computations were performed on a VAX based system in the Advanced Computational Laboratory of the Department of Aeronautics and Astronautics, Naval Postgraduate School.

B. OVERVIEW OF THESIS

The second chapter of the thesis covers background needed to understand chaos. The chapter begins with a short development of the mathematical basis for chaos. Probability theory, specifically the central limit theorem, is also developed. Then, the engineering techniques used to analyze chaos are presented. Pseudo phase planes, fractal dimension, Poincare' sections and Lyapunov exponents are presented here. Finally, the chapter ends with a literature review that discusses recent developments and relevant papers concerning

applications of chaos.

The third chapter begins with a discussion of a technique for simulating a continuous system using a digital computer. Next, the work of CDR Sarigul-Klijn is presented. Next, the methods used in the present analysis are presented. The multivariate scaling analysis is presented here. Further, the method used to analyze a continuous system using a discrete approximation is discussed.

Chapter IV presents a summary of the results of the analysis. First, the Lorenz equations and Duffing's equation are evaluated using current techniques. Next, the multivariate scaling analysis results are presented for the helicopter vibrations data.

Chapter V is a discussion of conclusions from the analysis. Scope for further research is also presented.

II. UNDERSTANDING CHAOS

A. INTRODUCTION

This chapter gives a brief overview of the background needed to understand the concept of chaos. First, the mathematical basis for chaotic dynamical systems is presented. Next, the engineering techniques used to analyze chaos are presented. Finally, the chapter ends with a review of recent literature that concerns applications of chaos that are relevant to the present study.

B. MATHEMATICAL BASIS FOR CHAOS

The study of chaotic systems begins with the study of discrete dynamical systems. Since data can only be collected at discrete points in time, it is quite natural to examine a dynamical system at those discrete points so that a model of the system can be constructed. The computer has allowed the analysis to be done with shorter and shorter time intervals. A simple example of a discrete dynamical system is an iterated function system constructed with a calculator. A value in this system depends on the previous value in the system. The system could be constructed by choosing a value and then repeatedly pressing the same function key on a calculator. If the key selected were the square root function and the starting number was 100, then we could construct a sequence of

numbers based on the function (square root) and the initial condition. Clearly this system is quite predictable but it is still dependent on the initial conditions. A system with this property is said to be deterministic.

Dynamical systems can be classified by the nature of the model that best describes that system. A 'linear' system is modeled by a function that is a straight line that passes through origin. A function is called 'affine' if its graph is a straight line that does not pass through the origin. An affine system could be modeled by the relationship:

$$X_{n+1} = AX_n + B.$$

A 'nonlinear system' takes the form:

$$X_{n+1} = f(X_n) + g(n)$$

where $f(X_n) = AX_n$ and $g(n)$ is a function of the iteration number. The graph of a nonlinear system is not a straight line and need not pass through the origin. For example, if $f(X) = x$ and $g(n) = n$ the equation for the 15th iteration would be

$$X_{15} = f(X_{14}) = X_{14} + 15.$$

A simple iterated function system might revisit a point after a certain interval. If $X_{n+1} = f(X_n) = X_n$ then X_n is called a 'fixed point'. If $X_n = f(X_n) = X_{n+m}$ then X_n is called a 'periodic point'. That is, if one starts at point X_n and performs 'm' iterations on the system the last iteration will yield point X_n . A fixed point remains fixed after successive

iterations, while a periodic point is revisited only after a certain number of function iterations.

Periodic points and fixed points can be classified as attracting or repelling. A point is called 'repelling' if a small perturbation in the initial condition causes the function to diverge exponentially. A point X is called attracting if a small perturbation in the initial condition causes the system to converge to point X after successive iterations. That is, if a system is iterated with two sets of initial conditions, one condition an attracting point and one condition ϵ distant from the attracting point, then after successive iterations the functional values will be closer together than the original points. Figure 2.1a and 2.1b exhibit a repelling point and an attracting point, respectively. It can be shown that if $|f'(X_n)| < 1$ then X_n is an attracting point. While, if $|f'(X_n)| > 1$ then X_n is a repelling point.

Before giving a somewhat generally accepted mathematical definition of chaos, the concepts of transitivity, denseness and other basic mathematical concepts must be explored. Many good references are available. Devaney [Ref. 2.1] presents a particularly good explanation of these mathematical concepts.

First the definition of metric space is presented. A 'metric space' (X, d) is a space X , together with a real valued function d , that maps points in X to points in X , and which

measures the distance between pairs of points in X . The function d must obey the following rules:

- (1) $d(x,y) = d(y,x)$ for all x and y in X
- (2) $0 < d(x,y) < \infty$ for all x, y in $X, x \neq y$
- (3) $d(x,x) = 0$ for all x in X
- (4) $d(x,y) < d(x,z) + d(z,y)$ for all $x, y,$ and z in X

A point is called a 'limit point' if there is a sequence of points that converge to that point. A connection between attractors and limit points becomes evident. The concept of convergence is common to both attractors and limit points. Next, the 'closure' of a subset of a metric space is said to be the union of that subset and all of its limit points. Next, 'denseness' is defined. Let (X,d) be a metric space. Let B be a subset of X . B is said to be dense in X if the closure of B equals X .

A set is 'closed' if it contains all of its limit points. If a set is not closed it is said to be 'open'. The concept of 'transitivity' is next presented. Let U and V be open subsets of the metric space (X,d) . A dynamical system $\{x,f\}$ in that metric space is transitive if there exists a finite integer such that

$$U \cap f^{on}(V) \neq \emptyset$$

In simple terms, this means that any arbitrarily small neighborhood in X will, under successive iterations, overlap

with any other arbitrarily small neighborhood in X . Therefore, the system cannot be divided into two disjoint open sets.

Now the definition of 'chaos' as defined in [Ref. 2.1] is presented. A system is said to be chaotic if:

- (1) it has sensitive dependence on initial conditions
- (2) it is topologically transitive
- (3) periodic points are dense.

An important phenomena in the study of chaos is the 'bifurcation'. In general, dynamical systems arrive at a chaotic state through a bifurcation of one type or another. Bifurcations are found throughout the real world. A bifurcation is simply a dramatic change in a dynamical system. Water freezing, beam buckling under loads and the splitting of an atom during a nuclear explosion are all examples of bifurcations. Many systems are nonchaotic until a parameter or set of parameters attain certain critical values. As the system achieves a critical state a bifurcation occurs and the system becomes chaotic. In general, not all bifurcations are identical.

A 'saddle-node bifurcation' occurs when a function has a semi-stable fixed point. A semi-stable fixed point is attracting if perturbed in one direction and repelling if perturbed in another direction. In the simplest two dimensional case, the bifurcation occurs as the function approaches

the line $y = x$. When the graph of the function just touches the line the function splits into two. Figures 2.2a and 2.2b provide graphical representations of a saddle-node bifurcation of the logistic equation.

A period doubling bifurcation occurs when an attracting fixed point becomes repelling. As the parameter achieves its critical value, the fixed point now becomes a cycle of period two. As the parameter passes another critical value, yet another split occurs. This process continues until a chaotic state is achieved. Saddle-node and period doubling are the two most common bifurcations. While others are found in nature, it is clear that a route to chaos is through bifurcations [Ref. 2.2].

A remarkable property about dynamical systems was proved by Sarkovskii [Ref 2.1]. Sarkovskii developed a procedure to determine the periods of a dynamical system. He showed that by ordering the integers in a certain manner, the periodic points of a function could be predicted. As previously discussed, a periodic point is a point that is revisited after a number of functions iterations. In this ordering if a system has a periodic point of a higher order period then it has periodic points of all the periods that follow. For example, if a system has a point of period three, then it has periodic points of all periods. To find points of other periods one must change the initial conditions. The highest order period is three and the lowest order period is one.

Sarkovskii's theorem states as follows:

let the ordering of the integers representing periodic points of a system be:

$$\begin{aligned}3 &> 5 > 7 > 9 \dots > \dots \\2 \times 3 &> 2 \times 5 > 2 \times 7 > \dots > \dots \\2^2 \times 3 &> 2^2 \times 5 > \dots > \dots \\2^5 &> 2^4 > 2^3 > 2^2 > 2 > 1\end{aligned}$$

then, if a function, f , has a periodic point of period n , and $n > K$ in the ordering, then f also has a periodic point of period K . Hence, period 3 implies all other periods. Period 2 only implies period 1.

The next concept to be discussed in this section, is the notion of a fractal. Fractals are subsets of metric spaces. Fractals have become important in helping to classify and quantify chaos. Fractal dimension is a useful tool in measuring chaos.

The mathematics behind the fractal is quite rigorous.[Ref.2.3] A basic example will present a clear picture of a fractal. The Cantor middle thirds set is the archetypical fractal. This set is constructed by starting with the interval $[0,1]$. The function removes the middle third of each remaining segment. After successive iterations the fractal remains. Figure 2.3 illustrates the Cantor set. What remains is the attractor for the system. Each segment is similar to the previous segment. This important property is called self-

similarity. The function for generating a fractal can be a rotation, a translation, a reflection or any combination of those three. Many functions or mappings may be needed to generate a particular fractal. In all cases, the function (or functions) acts on the previous point or segment. However, to generate a fractal each function must be contractive rather than expansive. This means that the function cannot enlarge the previous segment. But, the combination of multiple functions can be larger than the original segment.

'Fractal dimension' provides a useful measure of a chaotic system. A chaotic system will have a noninteger fractal dimension. While not all systems with noninteger fractal dimensions are chaotic, this is still a useful measure [Ref. 1.3].

The fractal dimension is a measure of how much space an object occupies in its metric space. An ϵ -ball about a point is simply all points less than ϵ distance from the point. To cover a set, one should take the smallest number of ϵ -balls that intersect all points in the set. The fractal dimension is defined as follows:

Let A be an element of the Hausdorff space where (X, d) is the metric. For each $\epsilon > 0$ let $N(A, \epsilon)$ denote the smallest number of closed balls of radius $\epsilon > 0$ needed to cover A .

$$D = \lim_{\epsilon \rightarrow 0} \frac{\ln(N(A, \epsilon))}{\ln(1/\epsilon)}$$

Then, element A is said to have fractal dimension D. The fractal dimension gives a measure of the relative size of the attractor of a chaotic system.

The examples discussed above were all one dimensional in nature. However, the concepts of chaotic dynamics can easily be applied to systems of higher dimensions.

The last concepts discussed in this section are the relevant areas of probability theory. The probability density function is the relative measure of the frequency of occurrences. For a discrete random variable the summation of all values of the probability density function is unity. That is, if $f(x_n)$ is the probability of occurrence of point x_n then

$$\sum_{n=1}^N f(x_n) = 1$$

This concept is intuitively obvious. The analog to summation for a continuous system is the integral; for a system with more than one random variable the concept does not change. For a multivariable system the summation over all random variables will equal unity. The summation over a single random variable of a multivariable system will always be less than or equal to unity.

Data can be distributed in a variety of patterns. If each value in the range has an equal probability of occurring, the data is said to have a uniform distribution. If the data is symmetrically dispersed about a central point with more data

near the center of the range than at the ends of the range, the data has a Gaussian or normal distribution. Figure 2.5 illustrates some common probability distributions. A key theorem allows data with any distribution to be transformed to normal distribution. The Central Limit Theorem follows:

Theorem: Let X_1, \dots, X_n be independent and identically distributed random variables all with expectations $= \mu$ and variance equal to σ

$$y_n = \frac{\bar{x} - \mu}{\sigma}$$

then Y_n converges to a standard normal random variable. This theorem is applied by Osborne and Provenzale [Ref 1.3] when comparing chaotic systems with randomly generated systems.

C. ENGINEERING TECHNIQUES

Most naturally occurring phenomenon have a continuous nonlinear pattern. To study these events, engineers must take discrete readings over a time interval or across a distance. The very act of measurement applies a strain on the system and slightly changes the system. The process of discretizing the continuous data produces an imperfect model of the system. Again error is introduced into the data. This section will discuss the engineering techniques used in the study of chaotic dynamics.

1. Time Domain Analysis

The three steps to convert an analog signal to a digital signal are sampling, quantizing and encoding [Refs. 1.2 and 2.4]. Sampling a continuous signal produces a series of discrete values. A generally accepted practice is to sample the data at twice the rate of the uppermost frequency of the signal. The sampled data must be quantized. The spectrum is divided into different levels known as quantum levels. The signal is then compared with each quantum level and the reading at a specific time is recorded at the nearest quantum level. The maximum error introduced here is then one-half the quantum level. The next step is translating the quantum levels to the maximum number of levels available in the data recording equipment. This is known as machine precision. Again an error is introduced into the data.

2. Frequency Domain Analysis

An alternative method for analyzing a continuous data signal is a frequency domain analysis. This method uses a Fourier analysis to measure a function using harmonic components that have varying amplitudes, frequencies and phases. A signal in the frequency domain can be represented by two plots. A power spectral density graph is a plot that is often used to represent signals. The square of the amplitude is plotted against the frequency.

3. Phase Planes and Pseudo Phase Planes

The concept of the phase plane was introduced by Poincare. A phase plane represents a dynamical system by using two independent properties that best describe the system dynamics. At each point in time those properties are measured and then plotted on a two dimensional graph. At any point in time the system can be described by a single point on the graph. The resulting plot is used to analyze the system. If the system approaches a limit point or limit cycle over time it is said to have an attractor. The phase plane requires two separate measurements of a system. As was discussed earlier, each measurement introduces an error into the data. Also, collecting data for two variables will be more costly and might be physically impossible. Hence, a phase plane analysis may be impractical.

Takens suggested a simpler technique for constructing a phase plane diagram [Ref. 2.5]. This technique is called a pseudo phase plane. A dynamical system is measured with only one variable. This procedure generates a single time series. A second time series is constructed by adding an embedding time to the original data. If the embedding time is two time periods, the third point in the original series becomes the first point in the new series. The data in the second series is then plotted versus the first series to construct a pseudo phase plane. The pseudo phase plane captures the system

dynamics without filtering the signal by integration or differentiation of the measured signals [Ref. 2.6]. Any dynamic property of the system can be used to represent the system. The choice of embedding values plays a critical role in the accuracy and interpretation of the analysis. A small embedding time produces a centralized data set while a large embedding time introduces error through edge effects.

Grassberger [Ref.2.7] suggests that the embedding time should be about one quarter of the most predominant frequency of the data. Dvorak and Klaschka [Ref. 2.8] have since proven that an embedding time between five and eleven time intervals produces a pseudo phase plane with the least amount of bias. In recent years, many methods have been developed for reducing the measurement error or noise in the analysis. Hammel [Ref. 2.9] has been able to reduce the effects of noise tenfold. This produces a data set that is accurate to machine precision on even the most advanced computers. For an experimental procedure or a numerical simulation, the pseudo phase plane is more efficient, less costly and produces results that are just as accurate as the phase plane and captures the original system dynamics.

Pseudo phase planes can be constructed in higher dimensions as well. The procedure to construct higher dimensional pseudo phase planes is similar to that used to construct the two dimensional phase planes. The third and subsequent time

series are constructed using the original time series and new embedding factors. The embedding factor should be different for each new time series. More than three dimensions cannot be depicted graphically but, multidimensional pseudo phase planes can provide insight into the dynamics of a system.

Poincare sections can be constructed from these phase planes [Ref. 2.10]. A Poincare section is a two dimensional cut of a three dimensional phase plane. The section shows where trajectories of the system pierce the phase plane. This section allows one to graphically determine if a bounded attractor or limit cycle is present. A well defined attractor is evidence of a chaotic system. The Poincare section can be taken at any angle so that the number of possible sections is infinite. Higher dimensional Poincare sections may be obtained similarly.

4. Van Der Pol Planes

In higher dimensional space, Poincare sections can be obtained as intersections of the trajectories with a specified hyper-plane. The internal structure of the attractor may then be examined. The Van Der Pol plot is constructed by untwisting the trajectory at a certain rate to create a series of Poincare sections. The sections are then merged together to yield a Van Der Pol plot [Ref. 2.11]. These are particularly useful when a single frequency dominates the response of a system. More information on Poincare sections can be found

in [Ref. 2.6].

5. Lyapunov Exponents

The methods discussed previously have all provided a graphical representation of the chaotic nature of dynamical systems. The graphs offer pictorial evidence of the chaotic nature of the system being analyzed. These methods do not provide quantitative measures of chaos. The Lyapunov exponent offers quantitative evidence of chaos. Wolf [Ref. 2.12] offers an algorithm for calculating these exponents based on a time series. This method measures the attraction or repulsion over time of two adjacent trajectories with different initial conditions. A positive exponent means that the distance between the systems has grown greater with time. A negative exponent indicates that the trajectories have grown closer. A positive exponent is an indication of unpredictability and chaotic behavior in a dynamical system. A positive exponent alone is not enough to determine if a system is chaotic. Recent studies by Kapitaniak and Naschie [Ref. 2.13] show that a purely random system can also have positive Lyapunov exponents.

The Lyapunov exponents also gives a measure of the rate of information loss in a system. As such, the exponent can be a useful gage as to how far into the future one can predict the dynamics of a system.

6. Fractal Dimension

Another measure used to quantify chaos in a dynamical system is the fractal correlation dimension. As discussed earlier, fractal dimension gives a lower bound for the number of degrees of freedom needed to model a physical system. A finite non-integer fractal dimension suggests yet further evidence of the presence of a strange attractor and chaos. However, Osborne and Provenzale have shown that a randomly constructed data can also have a non-integer fractal dimension [Ref. 1.3]. Ruelle [Ref. 2.14] has shown that all fractal dimension estimates that approach $2\log N$ are suspect. In this case, N is the number of data points the time series. Therefore, for most time series of 10,000 data points fractal dimension approaching six yields inconclusive evidence of chaos in the dynamical system.

As with much of this field, no universally accepted definition of fractal dimension exists as yet. Farmer et al [Ref. 2.15] describe seven natural measures of dimension that could be called fractal dimension. These measures can be divided into two broad classes. One class requires a probability measure to be computed. The other class requires only a geometric measurement.

7. Evolving Measures of Chaos

Osborne and Provenzale [Ref. 1.3] have suggested that a multivariate scaling analysis will lend additional insight into the dynamics of a system. A multivariate scaling

analysis involves computing probability density functions (PDF) of the time series data. The data is normalized before the PDF is constructed. A non-chaotic system will generate a Gaussian PDF. A chaotic system will yield a non-Gaussian PDF. These ideas will be further elaborated in Chapter III.

Lindsay [Ref 2.16] suggests a method for forecasting data points of a chaotic system. This method calls for calculating the Jacobian and strange attractor to use global rather than local properties of the attractor. A predictor function is constructed using the Jacobian that allows one to forecast as many as one-half the original number of data points.

The last two methods utilize the global properties of chaotic systems. Locally, random systems often mirror chaotic systems. A global approach helps to minimize the confusion caused when comparing local properties of random systems with local properties of chaotic systems.

D. SUMMARY

Techniques to analyze chaotic dynamical systems have emerged rapidly during the last decade. Mathematicians, physicists and engineers differ in their approach concerning analyzing the nature of chaotic systems. Methods to investigate chaos in systems modeled by differential equations are well documented. Such systems are continuous and need not be modeled with discrete data points. Measuring real physical systems yields discrete data points rather than continuous

equations. The measurement process introduces several sources of error into the system. Many methods can help describe the chaotic nature of such a system. But, as a result of the error introduced, no method gives a fool-proof description of chaos. Many techniques must be employed concurrently to ascertain the evidence of chaos and its associated properties that allow accurate definition of the dynamical system.

E. LITERATURE REVIEW

Researchers in the field of chaotic dynamics are breaking new ground daily and technical papers concerning chaos proliferate in leading scientific journals. In order to limit the scope of this literature review, the papers and reports discussed in this section are those that were published between December of 1989 and April of 1991. This list is not exhaustive, but covers the papers that are directly related to the subject matter of this thesis.

Bleher, Grebogi and Ott [Ref 2.17] have observed a new transition from a system in a steady-state to a system in a chaotic state. This transition is called an abrupt bifurcation. The abrupt bifurcation occurs in the context of chaotic scattering. The behavior is caused by the presence of a chaotic invariant set of unstable bounded orbits. An example showing the energy involved in atom-diatom collisions is discussed. Because of its dependence on a set of unstable bounded orbits, the abrupt bifurcation might help explain the nature of helicopter vibrations.

Hughes and Proctor [Ref.2.18] studied the effects of noise on a chaotic system. They show that noise, even at very low levels, can create great problems in determining the chaotic measures of a system. When noise was added to a known deterministic chaotic system the solution to the system is shown to be indeterminate and incomputable.

Corless, Frank and Monroe [Ref. 2.19] determine the chaotic properties of the Gauss map. The Gauss map is developed using continued fractions. The authors determine the fractal dimension, Lyapunov exponent and the correlation dimension of the continuous Gauss map. All of these properties indicate that the Gauss map is chaotic. Next, a numerical computer simulation is performed to generate a Gauss map. The simulated map has fractal dimension, Lyapunov exponent and correlation dimension that indicate the simulated system is nonchaotic. The simulated system is created to machine precision. The observable behavior of the systems is not significantly different. This suggests that a system with a long period might be chaotic.

A numerical experiment using a self-affine time series is presented by Higuchi [Ref 2.20]. The randomness of the phase distribution strongly affects the irregularity of the system. This conclusion is based on a comparison of the phase distribution with the fractal dimension. The randomness of the phase distribution is shown to be affected by the behavior of

the system in the time domain.

Liebert and Schuster [Ref. 2.21] report the effects of varying the embedding time delay when analyzing chaotic time series. For an infinite time series, any arbitrary value of an embedding value is acceptable when constructing a pseudo phase plane. However, for finite time series, arbitrary choices of embedding values can give erroneous results when calculating entropy and density. A method for calculating a proper embedding value which requires at least 9000 data points is presented.

Fang [Ref. 2.22] suggests that the interplay between a large noise intensity and the nonlinearity of the system may induce a nonequilibrium transition of the dynamical behavior of the system. The degree of distortion is based on the ratio of the noise intensity to a measure of the system nonlinearity. The chaotic measures of the system may be affected by that ratio. Specifically, the Lyapunov exponent changes sign as the noise level is adjusted. The system changes from a chaotic state to a periodic state with the introduction of strong white noise.

Kapitaniak [Ref. 2.23] presents a new method for estimating the parameter values that cause a dynamical system to be chaotic. This method applies to systems that exhibit a period doubling route to chaos. The method is applied to Duffing's oscillator. The method is based on an approximate analysis

and the Feigenbaum universal properties of period doubling.

Dvorak and Klaschka [Ref 2.8] present a modification to the Grassberger and Procaccia algorithm for finding correlation dimension. The original algorithm produces a bias for embedding dimensions greater than five. The correlation dimension of the system is changed because of the noise present in the algorithm. The new algorithm allows embedding dimensions up to eleven by reducing the white noise level. This algorithm removes the bias caused by the edge effects. All other causes of bias from the old algorithm are present in the new algorithm.

Chen and Ott [Ref 2.24] present an algorithm for computing the cross-sections of strange attractors. These cross-sections are useful for elucidating the geometry of the attractor. The cross-sections also allow one to estimate the fractal dimension of higher dimensional attractors.

Hammel [2.9] presents a method for reducing the noise of a time series of discrete data points. This method reduces the noise level tenfold. The reduction of noise allows one to distinguish the effects of noise from the effects of chaos. Both additive noise and dynamic noise levels are reduced. This method produces a time-series that is accurate to machine precision and thus yields more accurate calculations of chaotic measures of dynamical systems.

Stone [Ref 2.25] compares the effects of noise versus periodic forcing on the power spectra of a Duffing oscillator.

It is shown that the form of the power spectral density of the noise driven system and the deterministic chaotic system are indistinguishable. This suggests that a high frequency power spectrum cannot distinguish between a deterministic and stochastic system.

Lindsay [Ref. 2.16] presents a simple, computationally efficient method for forecasting chaotic time series using the Jacobian and certain weighting functions. The method requires solving a small number of linear equations. If the original time series has 10,000 data points, this method can calculate the next 5000 data points with exceptional accuracy. The error for the 5000th point is shown to be less than $2.7 \times 10^{-3}\%$. The same method can be used for noise reduction.

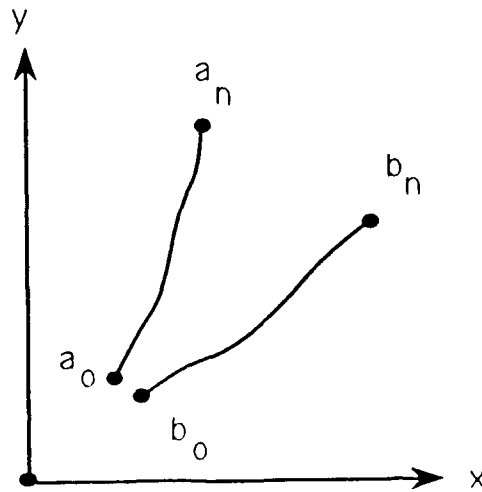


Figure 2.1a Repelling Point
 $\text{distance}(a_n, b_n) > \text{distance}(a_0, b_0)$

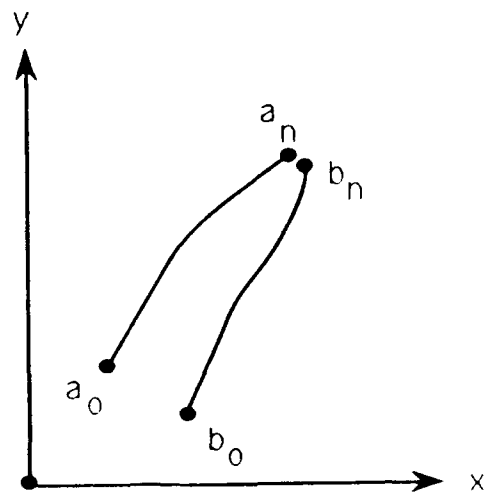
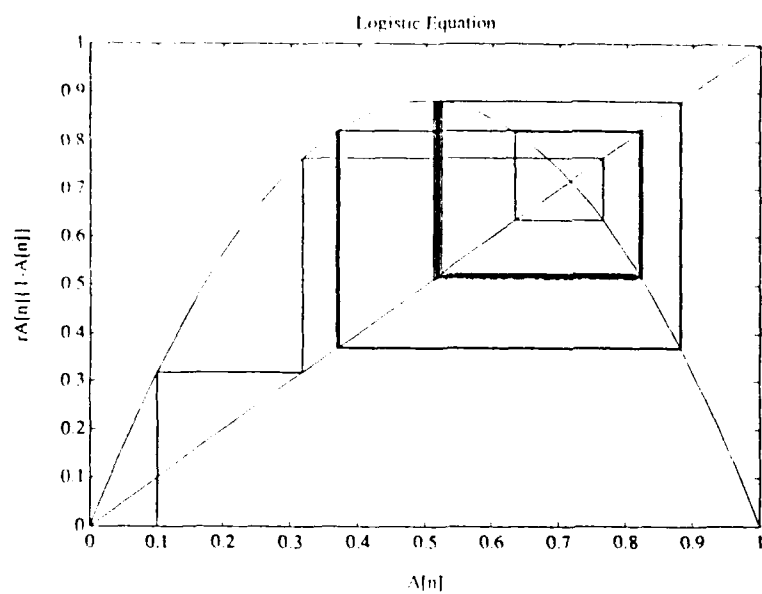
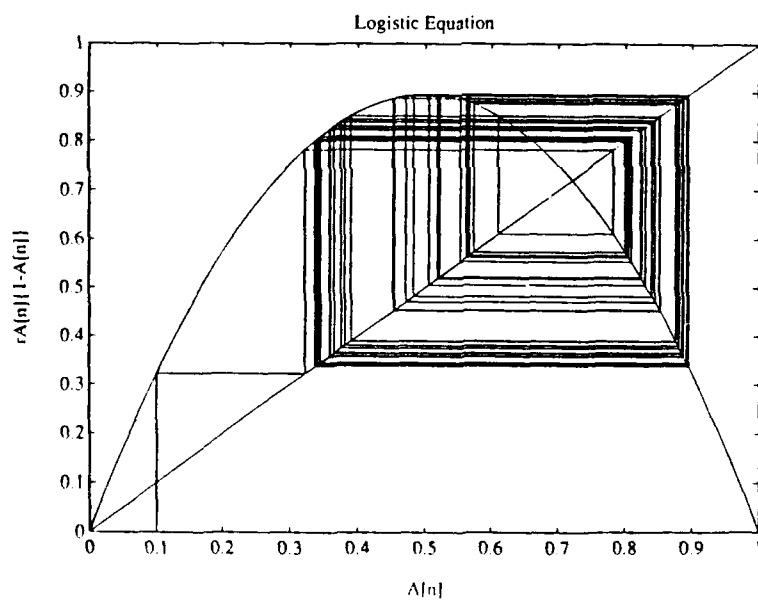


Figure 2.1b Attracting Point
 $\text{distance}(a_n, b_n) < \text{distance}(a_0, b_0)$



$$r = 3.54$$



$$r = 3.56$$

Figure 2.2 Period doubling route to chaos:
logistic equation $F(a) = r(a)(1-a)$

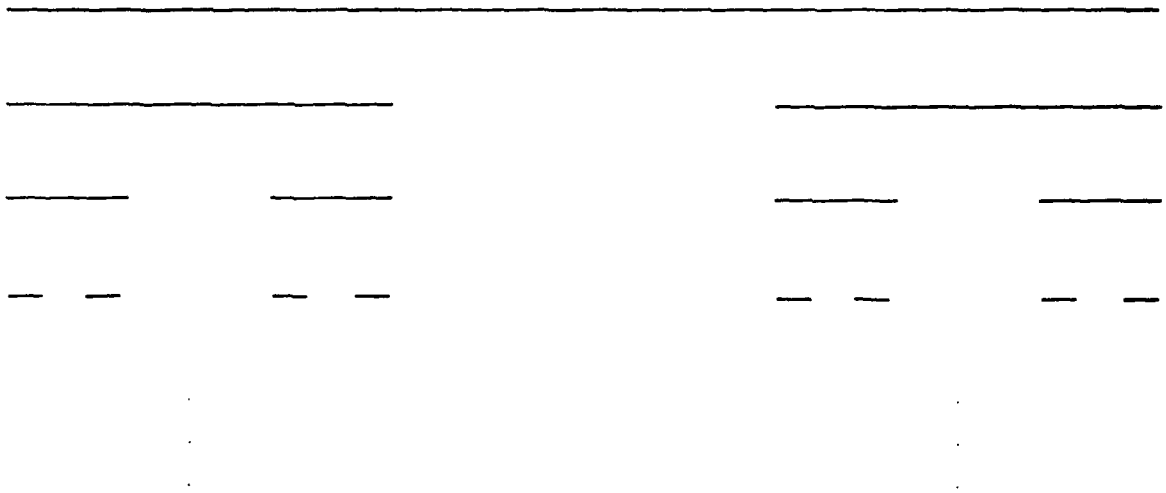


Figure 2.3
A Typical Fractal

III. METHODOLOGY

A. INTRODUCTION

This chapter presents the methods used to generate the simulated data and the methods used to study the nonlinear dynamical system data simulated and one set of helicopter flight vibration data. The first section presents the technique used to generate a discrete representation of a continuous system for the Lorenz equations and Duffing's equation. A discussion of randomly generated time series is also presented. Next, Sarigul-Klijn's work is discussed. This section focuses on the calculation of the fractal dimension and the Lyapunov exponent of a dynamical system represented by a time series. A development of the multivariate scaling analysis is then presented. The chapter closes with a review of the computer simulations used in the current analysis.

B. SIMULATING A CONTINUOUS SYSTEM

In 1963, Lorenz with the help of a computer, studied the atmosphere of a convecting fluid modeled by the now famous Lorenz equations.[Ref. 2.14] These equations were used

$$\frac{dx_1}{dt} = \sigma (x_2 - x_1)$$

$$\frac{dx_2}{dt} = \rho x_1 - x_2 - x_1 x_3$$

$$\frac{dx_3}{dt} = -\beta x_3 + x_1 x_3$$

where

σ is the Prantl number

ρ is the Rayleigh number

β is the aspect ratio.

Lorenz studied these equations with the following combination of parameters

$$\sigma = 10$$

$$\rho = 28$$

$$\beta = 8/3$$

used to model the system. Lorenz argued that the atmosphere modeled by this system of equations is chaotic and therefore, with current methods longterm behavior could not be predicted. The earth's atmosphere is similar to the system modeled by the Lorenz' equations and thus, longterm weather patterns are also unpredictable. Lorenz used the term chaotic to mean that the system had sensitive dependence on initial conditions. In 1980, Ueda [Ref. 3.1] studied the Duffing equation to model the motion of a system with a forcing function undergoing

large elastic deflection. Ueda found that the time series generated from the behavior of this equation

$$\frac{d^2x}{dt^2} + 0.05 \frac{dx}{dt} + x^3 = 7.5 \cos(t)$$

also exhibited chaotic tendencies. That is, a long term prediction about the behavior of the system is impossible. Both Duffing's equation and the Lorenz equations are models of continuous dynamical systems. These equations also model the dynamics of several systems.

To effectively analyze these systems with a digital computer a time series of discrete data points is needed. In the present study, a fourth order Runge-Kutta numerical integration was used to generate the time series. Many excellent references are available for this and other numerical integration schemes [Refs. 3.2 and 3.3]. The fourth order Runge-Kutta technique was used because it provided the level of precision required for the analysis. An adaptive step size control procedure was not used because the adaptive strategy is not compatible with the use of an embedding technique for generating a pseudo phase plane. To accurately generate a pseudo phase plane the original time series should have uniformly spaced data. Adaptive step size does not provide evenly spaced data and therefore was impractical for the current analysis. Acceptable precision was achieved by using a step size of .01 seconds. The equation parameters, step

size, embedding dimension and initial conditions were all varied to generate different time series for analysis. The time series were then analyzed.

Normally distributed colored random noise was numerically simulated using a random number generator. The generator yielded uniformly distributed random numbers. The Central Limit Theorem was applied to those numbers to generate a series of normally distributed numbers. Twelve uniform random numbers were used to produce one Gaussian random number [Ref. 3.4]. The numbers were then added to a sine function to produce a time series of simulated colored noise. The equation used to generate the series is

$$X = .9 + .25\sin(2\pi) + .1RAND$$

C. AN OVERVIEW OF SARIGUL-KLIJN'S WORK

Sarigul-Klijn performed an analysis of helicopter flight vibration data [Ref. 1.2]. This section is a brief description of part of his work. Although helicopter vibrations are mostly periodic, evidence of chaos was claimed. Specifically, the Lyapunov exponent for the vertical acceleration measured under the pilot's seat was found to be 0.3 to 1.7 bits per second. Also, the fractal dimension for this data was found to converge to 6.6 as the embedding dimension was increased. The fractal dimension for the lateral and longitudinal accelerations converged to 6.3 and 6.4, respectively. A random signal was found to have a linearly increasing fractal

dimension. This random signal had uniform distribution, instead of the more widely used normal distribution.

The Lyapunov exponents were calculated based on an algorithm developed by Wolf et al. [Ref. 2.12]. The exponent is defined as follows

$$\lambda = \log_2 \left(\frac{d(t)}{d(0)} \right)$$

where

$d(0)$ is the initial distance between trajectories

$d(t)$ is the distance at time 't'

The algorithm measures the distance between points in the original time series and the points in the embedded time series. A positive exponent for any measurable observable indicates diverging separation between trajectories and hence evidence of chaos.

Sarigul-Klijn adopted the method attributed to Grassberger and Procaccia to calculate fractal correlation. This is one of many measures of fractal dimension [Ref. 2.15]. This measure of fractal dimension is defined as follows:

$$C(r) = r^d$$

where

$C(r)$ is the probability of the attractor within a ball
of radius r (r -ball)

r is the radius of the ball

d is the fractal dimension.

Therefore

$$d = \lim_{r \rightarrow 0} \left(\frac{\ln C(r)}{\ln r} \right)$$

The fractal correlation dimension is computed by dividing the number of points inside the r -ball by the total number of points in the attractor. The process is repeated for several values of ' r '. The slope of the $\ln C(r)$ versus $\ln r$ curve gives the value of the fractal correlation dimension.

The fractal dimension is obtained by applying this procedure to all dimensions of the pseudo phase space. As the phase space dimensions increase, the correlation dimension will approach an asymptotic value. For chaotic systems, this value should be a finite noninteger value.

D. MULTIVARIATE SCALING ANALYSIS

This section presents the multivariate scaling analysis proposed by Osborne and Provenzale [Ref. 1.3]. Osborne and Provenzale found that a stochastic process, simple colored

random noise, can have a finite fractal correlation dimension. Previously, a finite fractal correlation dimension was thought to be positive indication of the presence of chaos. A new method, the multivariate scaling analysis, was developed to aid in the search for chaos.

The analysis begins with a time series of data. A second time series is generated with an embedding procedure or by taking a second measurement of the same variable. In the present analysis, a time embedding procedure was used to generate the second time series. The two time series are used to construct a scaling space. The coordinates for the scaling space are generated as follows

$$s_n(t_{(i-1)M+j}) = x_n(t_i) - x_n(t_j), \text{ for } i \neq j \quad (12)$$

where

s_n are the scaling space coordinates

$x_n(t_i)$ is the original time series

$x_n(t_j)$ is the embedded series

M is the number of points in the original series.

Since the points where $i \neq j$ are not used, the time series of scales will have $M^2 - M$ data points. The embedding dimension determines how many sets of scaling coordinates are generated. The dimension of the scaling space is equal to the embedding dimension. If the embedding dimension is two, then two sets of scaling coordinates are generated. A second series of scaling coordinates is constructed using the same procedure

but a different embedding value than the first series. A joint probability density function is then constructed using the procedure discussed in Chapter II. This process can be applied to create a scaling space of two or higher dimensions. However, a graphic analysis only allows two dimensions to be viewed. The probability density function is analyzed to determine the chaotic nature of the system. A nonchaotic system will yield a joint probability density function that is Gaussian or nearly Gaussian in nature. A chaotic system will yield a joint probability density function that is clearly nonGaussian in nature.

In the present analysis, multivariate scaling spaces and joint probability density functions were constructed for the Lorenz equations, Duffing's equation, helicopter vibration data and colored random noise. While the multivariate scaling analysis does not provide conclusive proof of the presence of chaos, it does provide evidence to support a thorough investigation of a dynamical system.

E. COMPUTER SIMULATIONS

The analysis of data was conducted using the methods described in previous sections. Time series were numerically generated for the Lorenz equations, Duffing's equation and colored random noise. Many different parameter values were studied for the Lorenz and Duffing's systems. Different values of step size were tried for the numerical integrations. For all cases, effect of changes in embedding value was

studied. Lastly, for all cases, various sets of initial conditions were evaluated.

The evaluations consisted of observing time history, computing fractal correlation dimension, Lyapunov exponents, Fourier spectrum and conducting a multivariate scaling space analysis for each set of parameters, embedding values, initial conditions and step size. Each variable could conceivably affect the chaotic nature of the system. Significant results are presented in Chapter IV.

IV. RESULTS

A. INTRODUCTION

This chapter presents the results of the analysis of the Lorenz equations, Duffing's equations, random colored noise and helicopter flight vibration data. The results are first presented for each dynamical system. In order to study the dynamical system described by a system of ordinary differential equations, a program was developed based on a 4th order Runge-Kutta integration scheme. The program generated the time dependent information necessary to study the dynamical system. Another program, based on the multivariate scaling analysis, uses the time histories to compute joint probability density functions as discussed in earlier chapters. Listings of these programs are included in Appendices A and B, respectively.

B. RANDOM COLORED NOISE

Random colored noise is generated using the following equation:

$$X = .9 + .25\sin(2\pi) + .1\text{RAND}$$

The data generated is normalized to yield a Gaussian

distribution. A comparison of fractal correlation dimension for random colored noise and purely random data is included as Figure 4.1. The number of points generated is 10,000 with an embedding time of 10 samples. The fractal correlation dimension of the random data increases linearly to infinity with the embedding dimension. The fractal correlation dimension of the random colored noise increases at a slower rate than the embedding dimension and appears to reach an asymptotic limit. The fractal dimension of random colored noise is a noninteger finite number for all values of embedding dimension that were tested. This data supports the conclusion of Osborne and Provenzale [Ref. 1.3]. A multivariate scaling analysis of random colored noise yields a joint probability density function that is seen to be Gaussian in nature. A graph of this function is included as Figure 4.2.

C. LORENZ EQUATIONS

The time series for the Lorenz equations is numerically generated using a fourth order Runge-Kutta integration numerical scheme. Step sizes of .001 seconds, .01 seconds and 0.1 seconds were used. This system of equations could not be solved, even using double precision arithmetic, with a step-size of greater than .115 seconds on either the Micro-VAX II computer at the Naval Postgraduate School or the CRAY-YMP computer at NASA-Ames Center. Step sizes larger than .115

caused an arithmetic overflow error. Hence, all computations were performed with step-sizes less than .115 seconds. Figure 4.3 shows a comparison of the X-Z phase plane with a pseudo phase plane generated using the X time series only and an embedding value of one. 10,000 data points were used to generate the pseudo phase plane. The pseudo phase plane has the same general structure as the phase plane with a rotation of one branch of the diagram. Larger embedding dimensions caused the psuedo phase plane to rotate and generate more branches. The fractal correlation dimension increases with step size. Figure 4.4 shows a comparison of fractal dimension to step size. A step size of .1 seconds yields a fractal correlation dimension of 2.04 which agrees with the work of Grassberger and Procaccia [Ref. 4.1]. Figure 4.5 shows plots of the slope of the $\log(r)$ versus $\log C(r)$ curve with differing step sizes.

An interesting result was observed as the Lorenz equations were studied. Smaller step sizes resulted in a loss of low frequency cycles in the Fourier spectrum. Figure 4.6 shows the Fourier spectrum plotted to the Nyquist frequency for the differing step sizes. Figure 4.7 shows plots to 20% of the Nyquist frequencies. Figure 4.8 shows the low frequency Fourier spectrum for different step sizes. The smaller step size appears to act as a filter for the low frequency components of the Fourier spectrum. The multivariate scaling analysis, using a 10,000 data points and a time delay of one

sample, exhibited a non Gaussian behavior suggesting a chaotic attractor [Ref 1.3]. The probability distribution function is included as Figure 4.9.

D. DUFFING'S EQUATIONS

Next Duffing's equation, which is known to exhibit chaotic behavior is studied. Numerical solution was obtained by adapting the program developed for the Lorenz equations. Figure 4.10 shows a comparison of the X-Y phase plane versus the pseudo phase plane generated with an embedding dimension of 1 applied to the X time series. Again, fractal correlation dimension changed with step size. However, in this case the fractal dimension decreased with larger step sizes. In all cases, the fractal correlation dimensions were finite non-integer values. The range of fractal dimensions agrees with the work of Moon and Li [Ref. 4.2]. Figure 4.11 shows a comparison of fractal dimension versus change in step size using 10,000 data points with an embedding dimension of 10 and a time delay of 1 sample. Figure 4.12 shows the Fourier spectrum plotted to the Nyquist frequency for the various step sizes. Figure 4.13 shows the Fourier spectrum plotted to 20% of the Nyquist frequency. Figure 4.14 shows a comparison of step size versus the low frequency Fourier spectrum. Again, the smaller step size acts as a low pass filter. But in this analysis the larger step size appears to cause the data to have quasiperiodic behavior. Figure 4.15 shows a graph of the joint probability density function generated from the

multivariate scaling analysis. The graph is seen to be non-Gaussian indicating chaotic behavior.

E. HELICOPTER VIBRATION DATA

This section presents an application of the multivariate scaling analysis based on the pseudo phase plane method for the helicopter vibration data [Ref. 1.2]. The vibration data selected for the present study are the vertical acceleration recorded under the right pilot seat of an OH-6A helicopter. Both Higher Harmonic Control 'off' and 'on' are studied. The joint probability density function with a time delay of 10 data points is included as figure 4.16. The graph differs little from a standard Gaussian distribution. The variation is more like the random colored noise than Lorenz or Duffing's equations. Figure 4.17 shows the joint probability density functions for all of the dynamical systems studied. This suggests that part of the helicopter vibrations are periodic while part of the vibration is chaotic. This conclusion supports the work of Sarigul-Klijn [Ref 1.2].

F. CONCLUSIONS

Two trends are evident in the analysis of the data. It appears that integration step size filters the data generated by numerical integration using a computer. Small step sizes might cause a loss of the low frequency components while large step sizes could cause the behavior of a chaotic dynamical system to appear to be quasiperiodic. The multivariate

scaling analysis appears to give an indication of the chaotic nature of a dynamical system distinguished from random data. Still, in the search for chaos, this technique probably does not provide a definitive answer as to the nature of chaotic behavior.

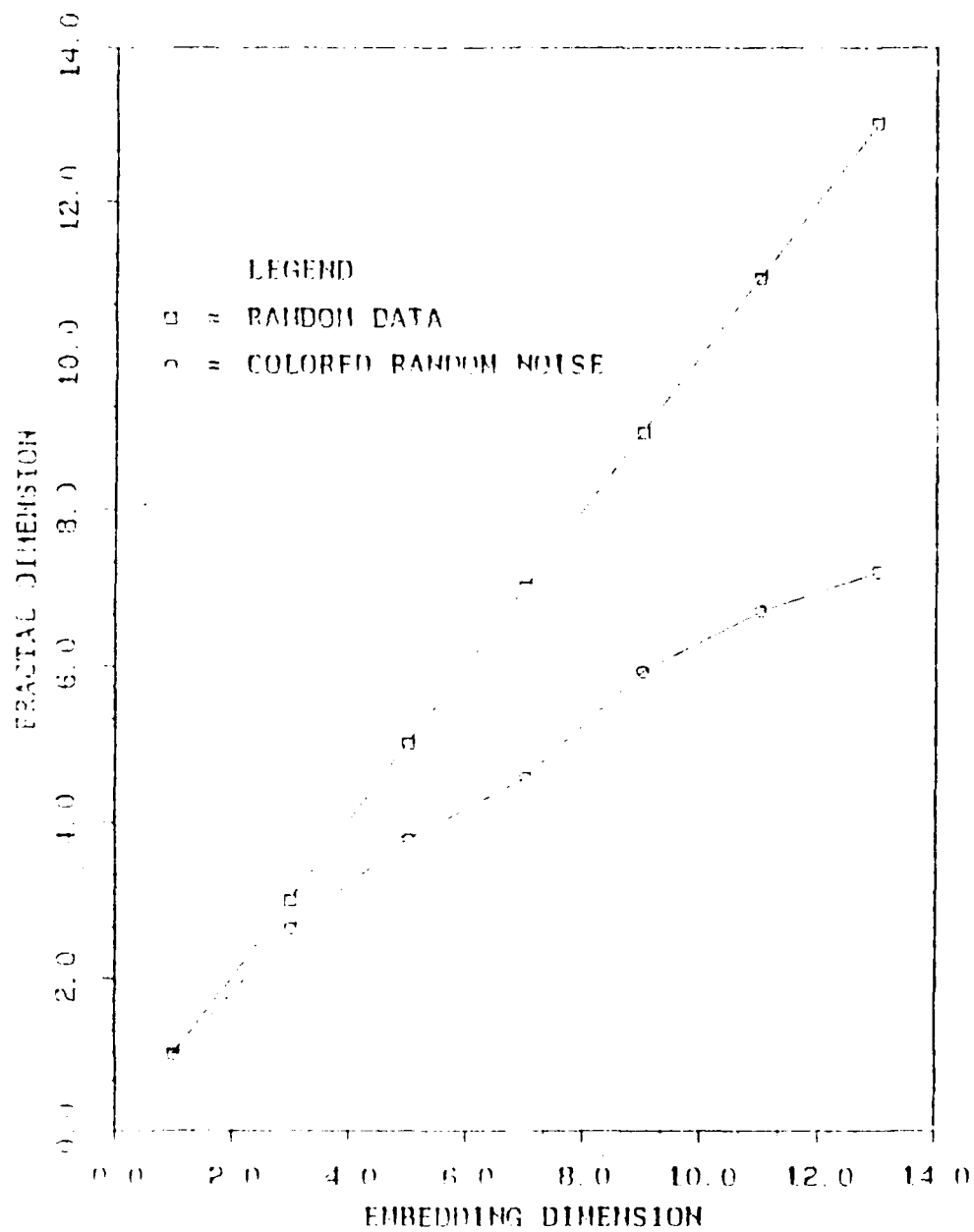


Figure 4.1 Fractal dimension vs. embedding dimension for random data and random colored noise.

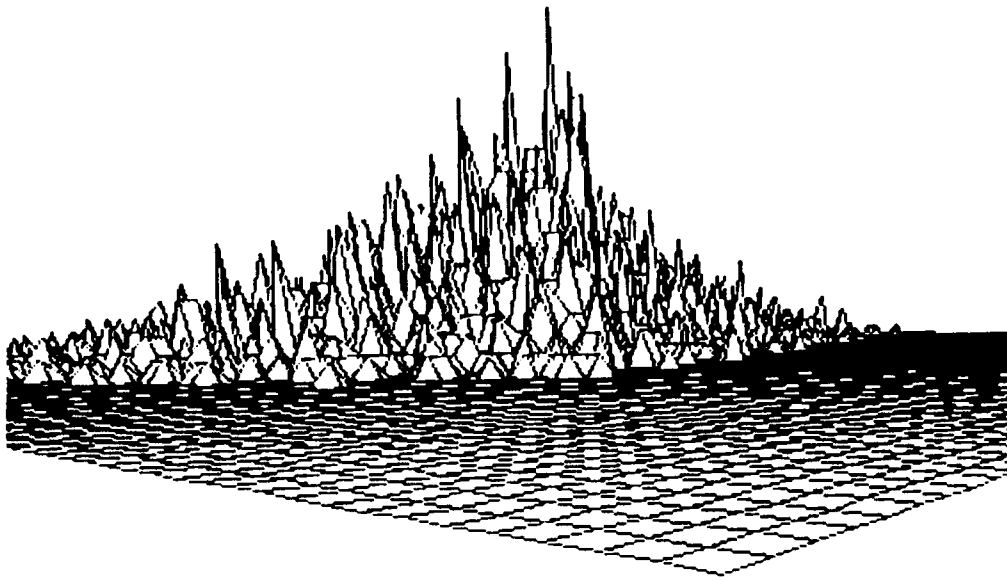


Figure 4.2 Joint probability density function for 2-D scaling space generated from random colored noise using a multivariate scaling analysis.

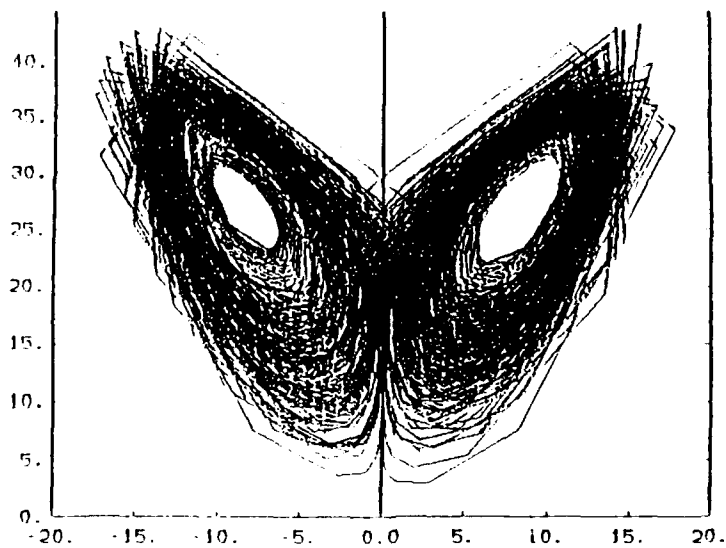


Figure 4.3a X-Z phase plane generated from Lorenz equations.

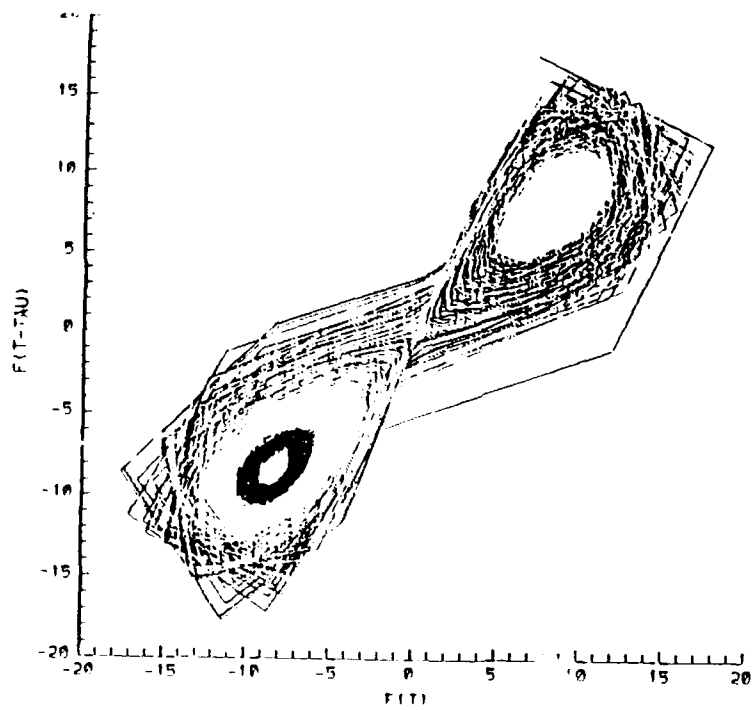
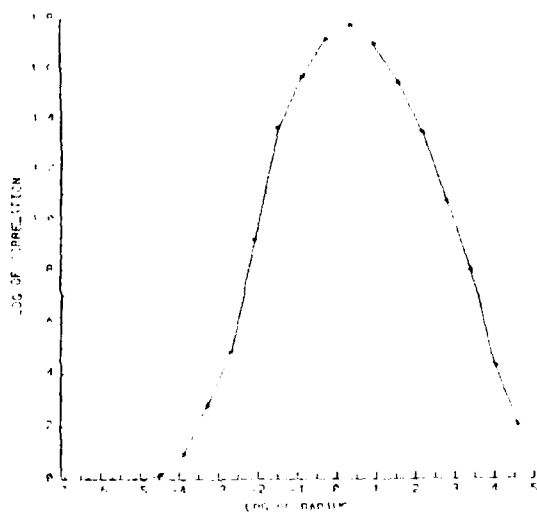


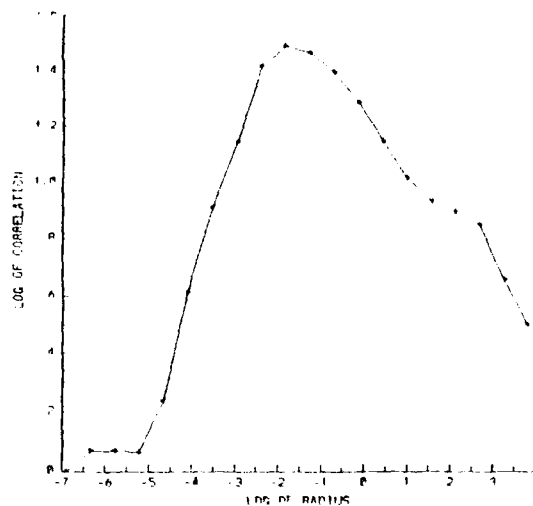
Figure 4.3b X-x pseudo phase plane generated from equations.

	step size	fractal dim.
LORENZ	.1	2.04
	.01	1.80
	.001	1.55
DUFFING'S	.1	1.35
	.01	1.35
	.001	1.60

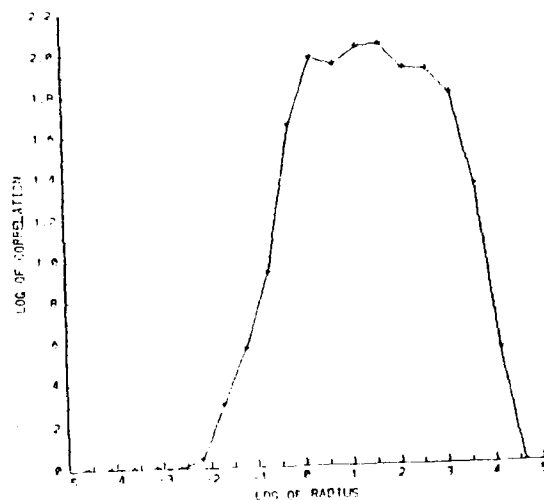
Figure 4.4 Fractal dimension vs.
step size



step size = .01 sec

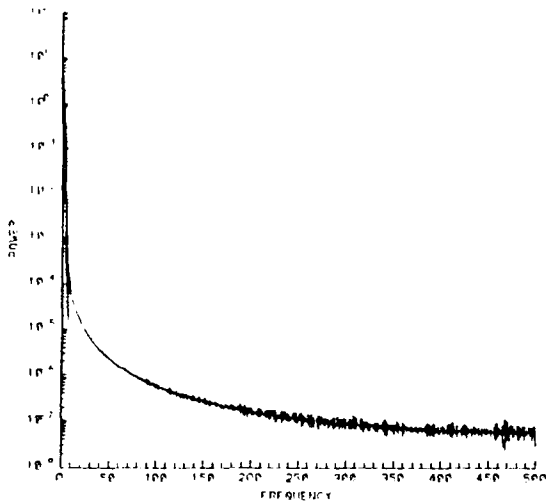


step size = .001 sec

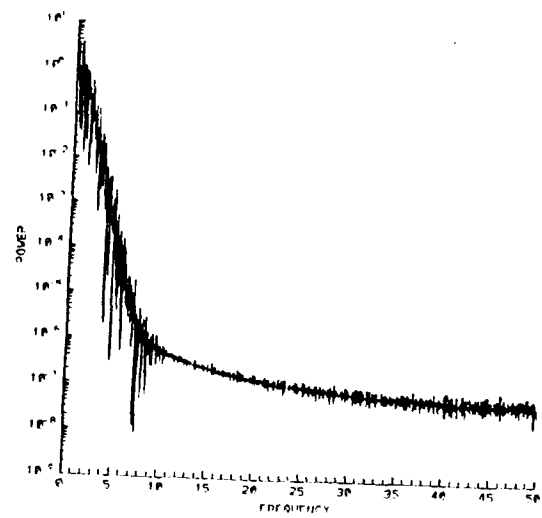


step size = .1 sec

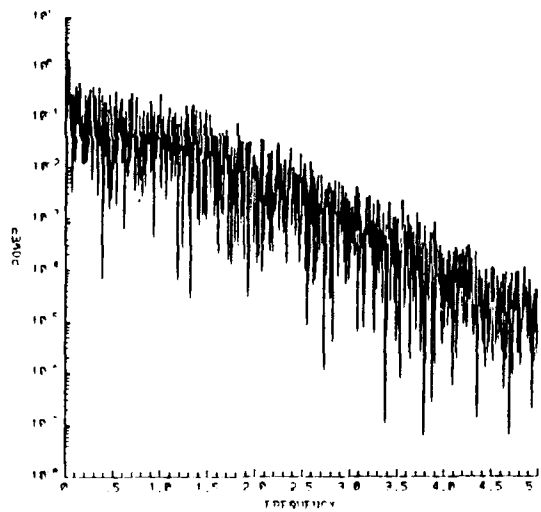
Figure 4.5 Slope of $\log(r)$ vs. $\log C(r)$ for Lorenz equations. Maximum point is fractal correlation dimension.



step size = .001 sec

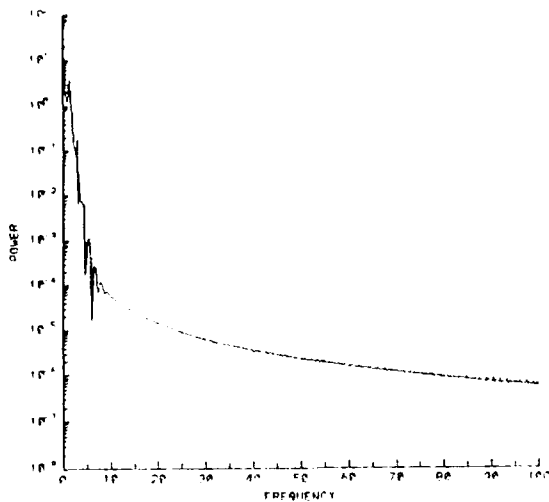


step size = .01 sec

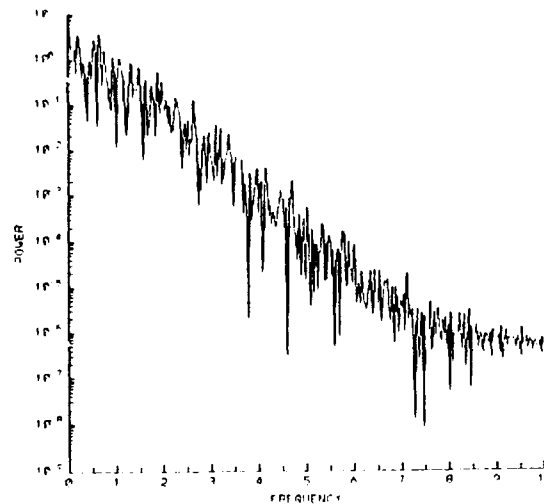


step size = .1 sec

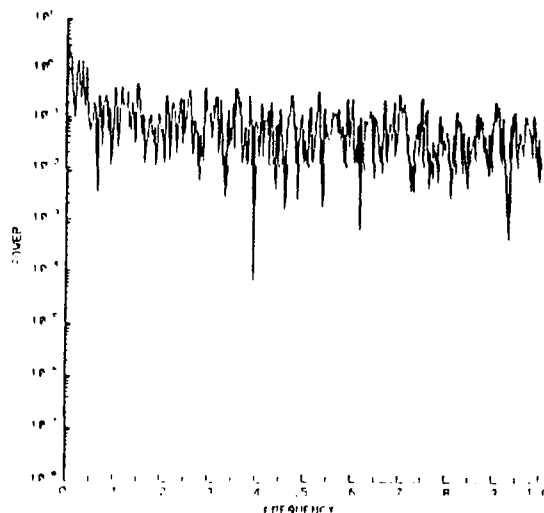
Figure 4.6 Fourier spectrum for the Lorenz equations plotted to the Nyquist frequencies.



step size = .001 sec

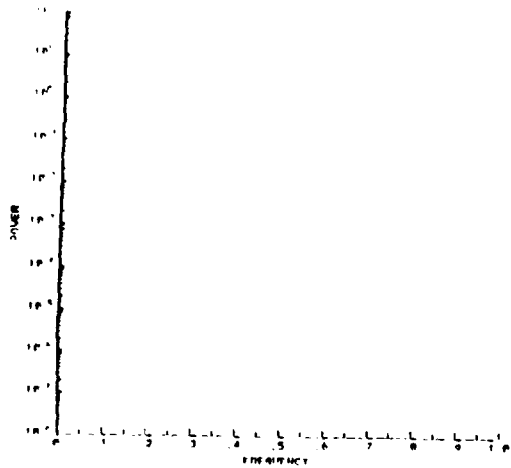


step size = .01 sec

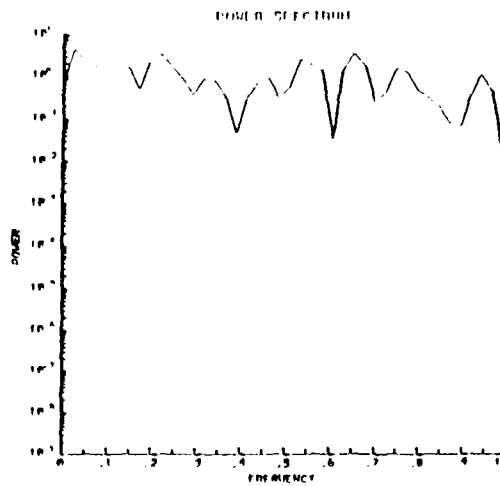


step size = .1 sec

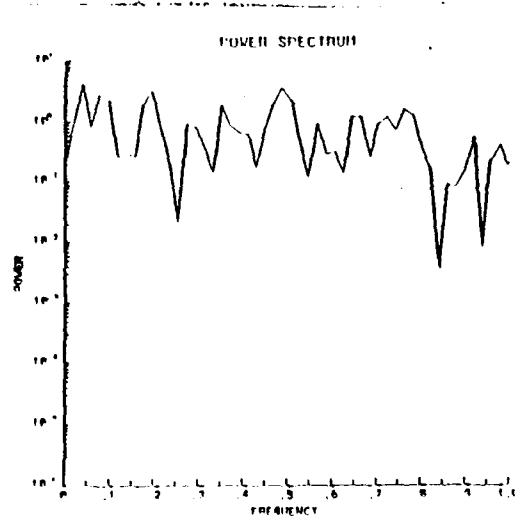
Figure 4.7 Fourier spectrum for the Lorenz equations plotted to 20% of the Nyquist frequencies.



stepsize = .001 sec



stepsize = .01 sec



stepsize = .1 sec

Figure 4.8 Low frequency Fourier spectrum generated from Lorenz equations.

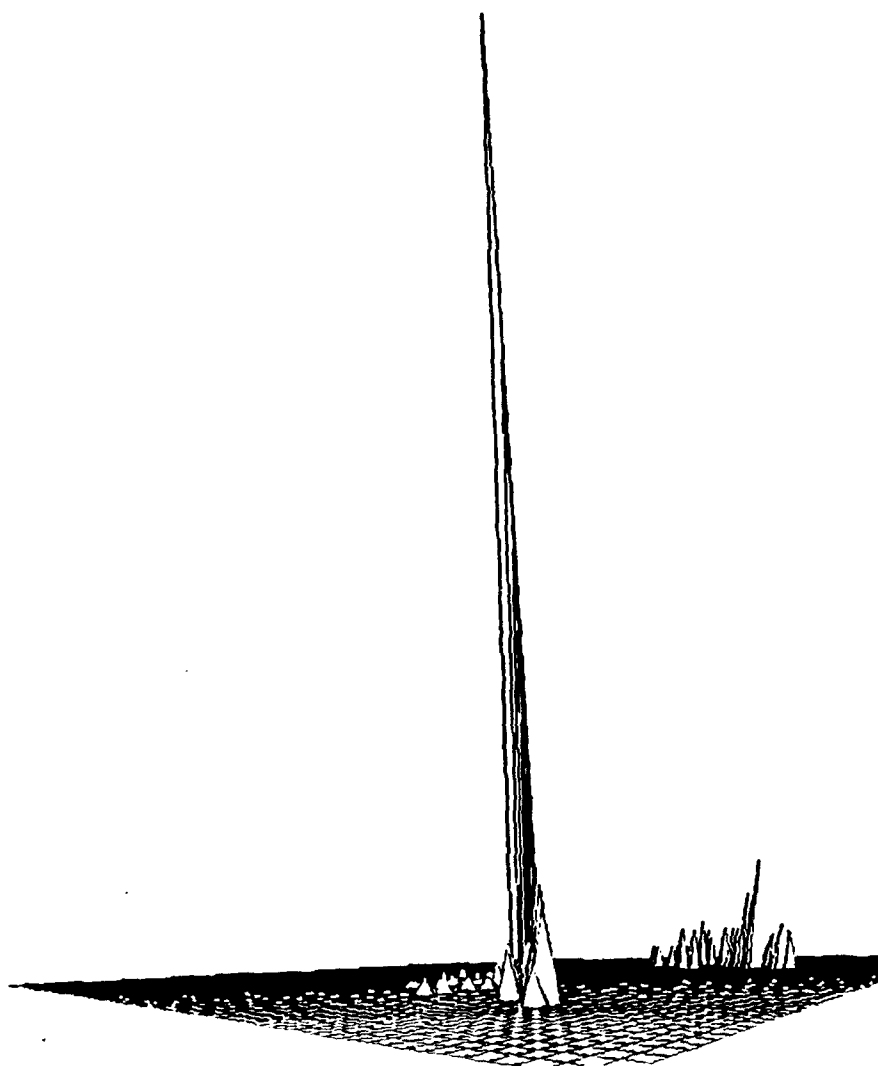


Figure 4.9 Scaling space joint probability density function for the Lorenz equations.

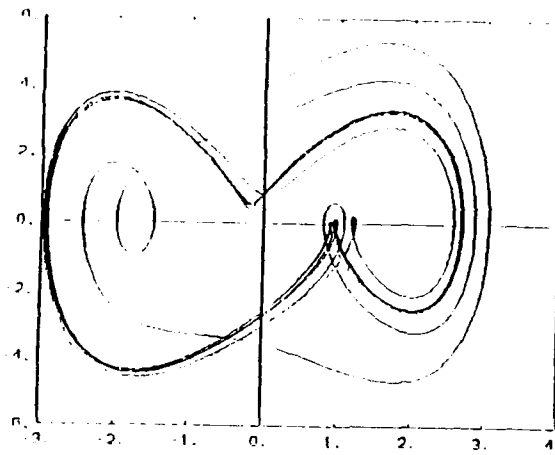


Figure 4.10a X-Y phase plane for Duffing's equation.

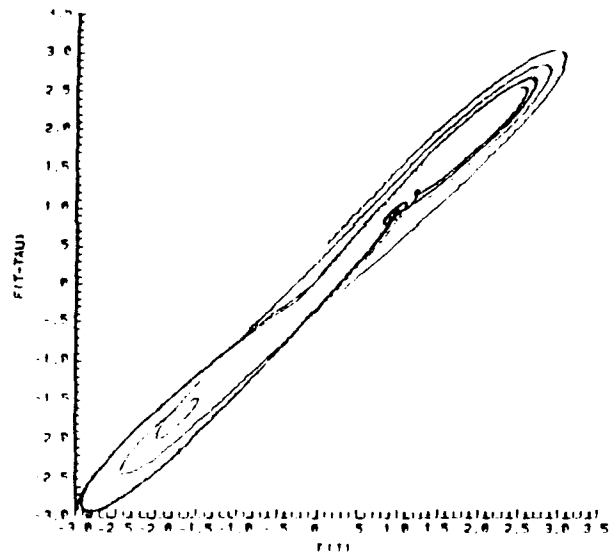
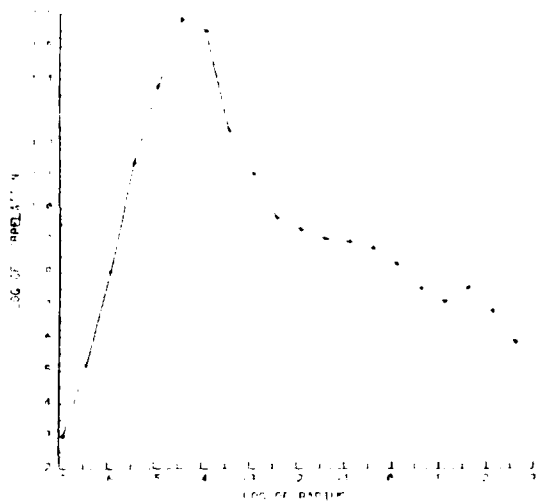
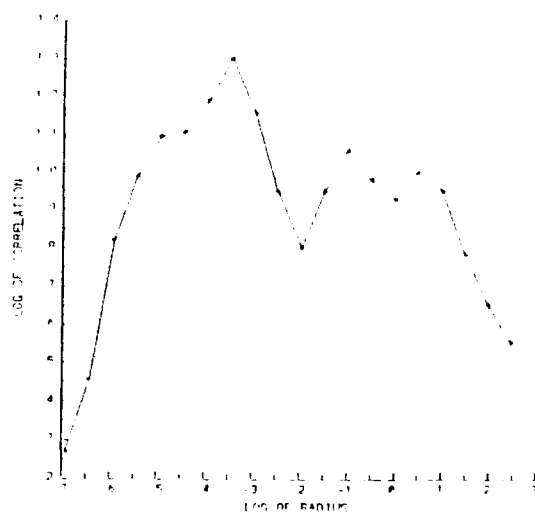


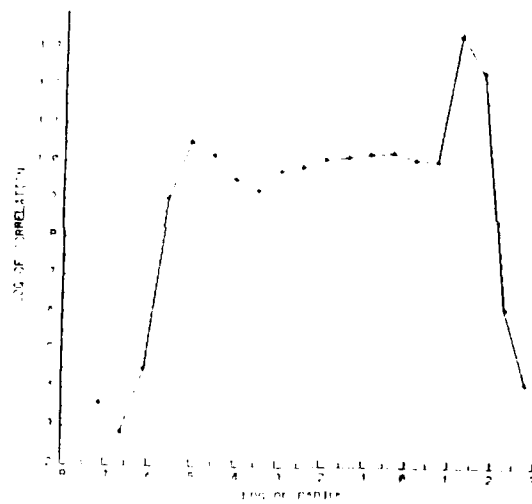
Figure 4.10b X-X pseudo phase plane for Duffing's equation.



stepsize = .001 sec

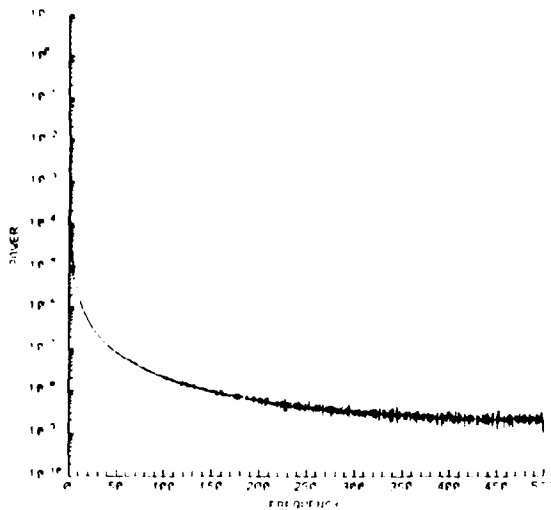


stepsize = .01 sec

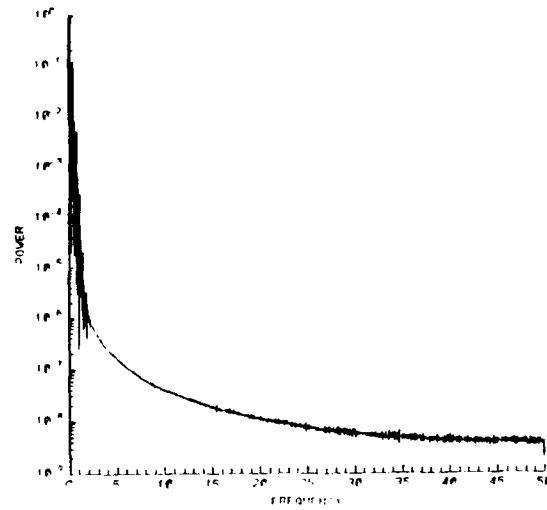


stepsize = .1 sec

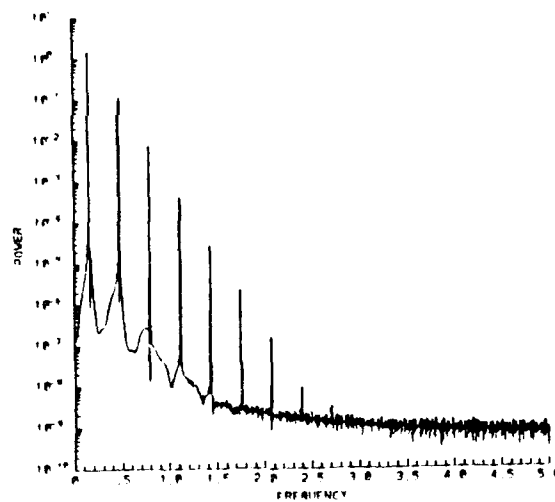
Figure 4.11 Slope of $\log(r)$ vs. $\log C(r)$ for Duffing's equation. The maximum point on the curve is the fractal correlation dimension.



step size = .001 sec

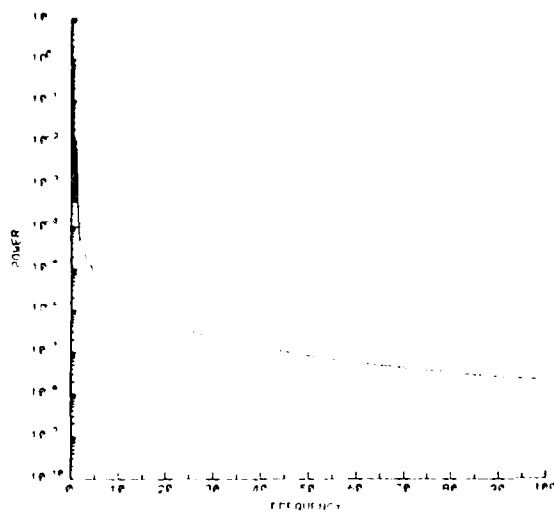


step size = .01 sec

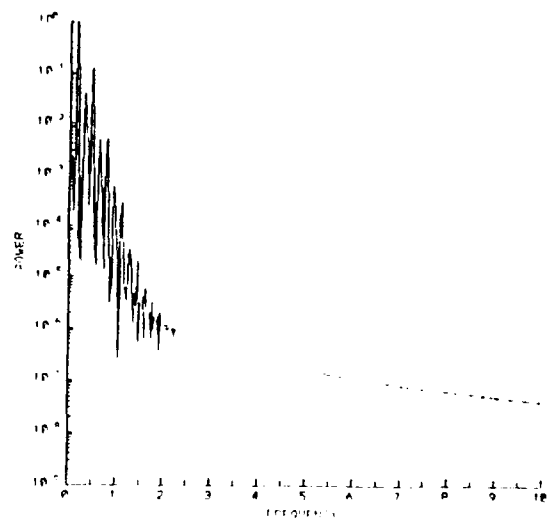


step size = .1 sec

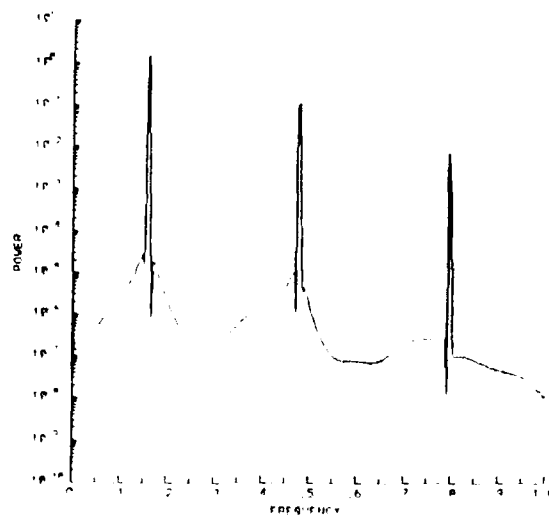
Figure 4.12 Fourier spectrum plotted to the Nyquist frequency for Duffing's equation.



step size = .001 sec

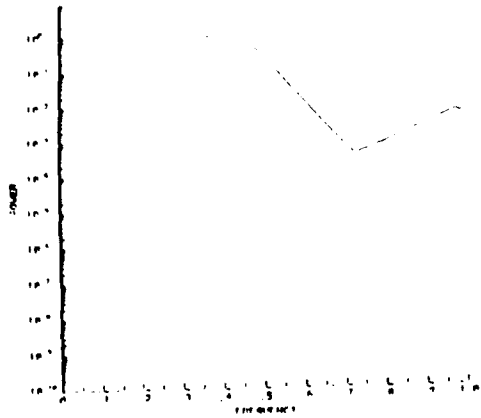


step size = .01 sec

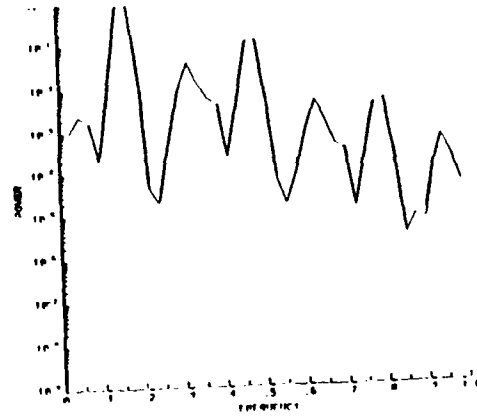


step size = .1 sec

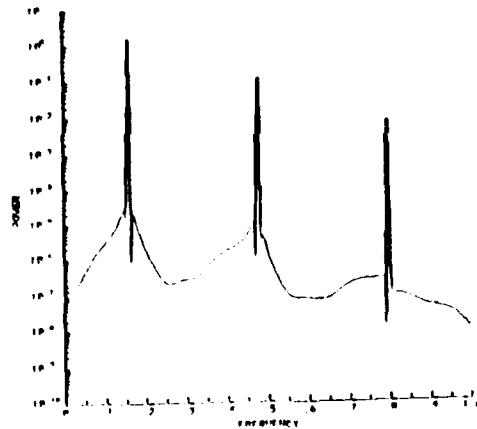
Figure 4.13 Fourier spectrum for
Duffing's equation plotted to
20% of the Nyquist frequency



stepsize = .001 sec



stepsize = .01 sec



stepsize = .1 sec

Figure 4.14 Low frequency Fourier spectrum for Duffing's equation.

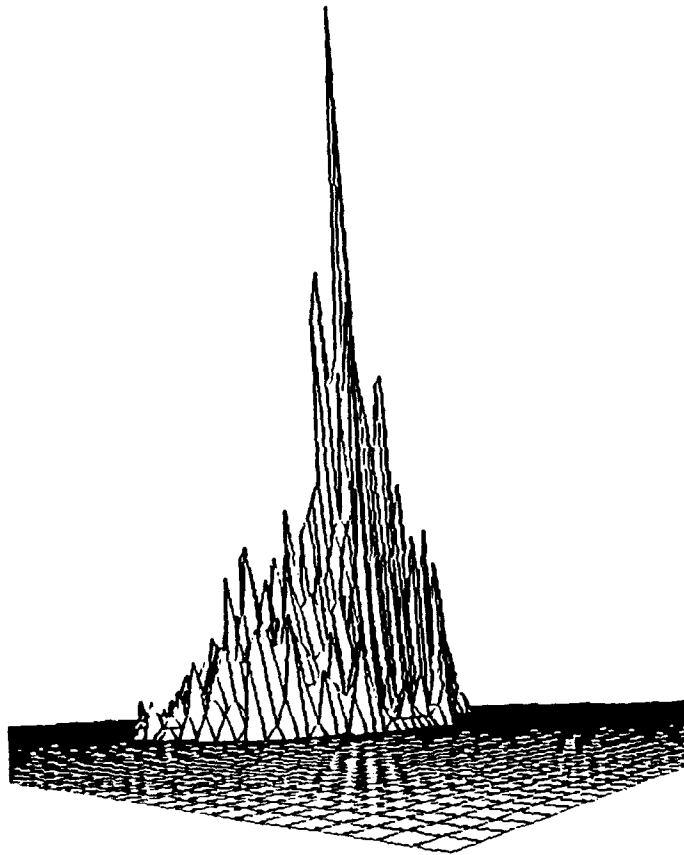


Figure 4.15 Joint probability density function for scaling space for Duffing's equations.

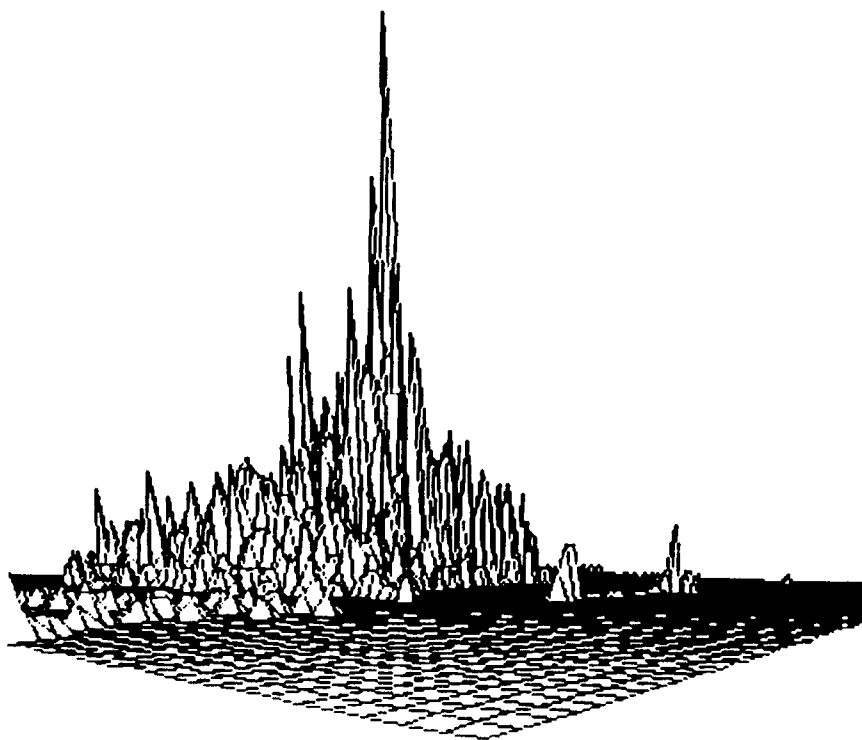
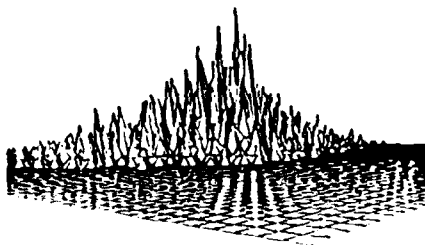
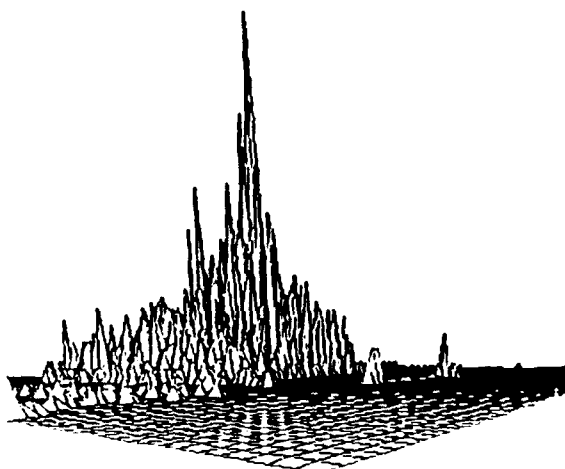


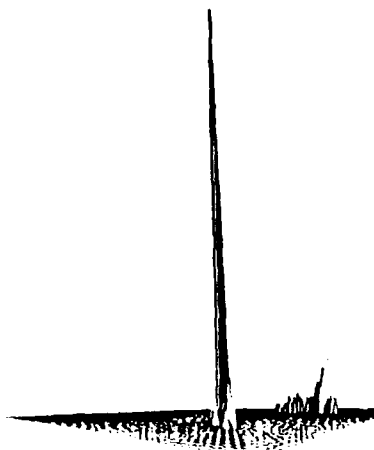
Figure 4.16 Joint probability density function for scaling space for helicopter vibration vertical acceleration data.



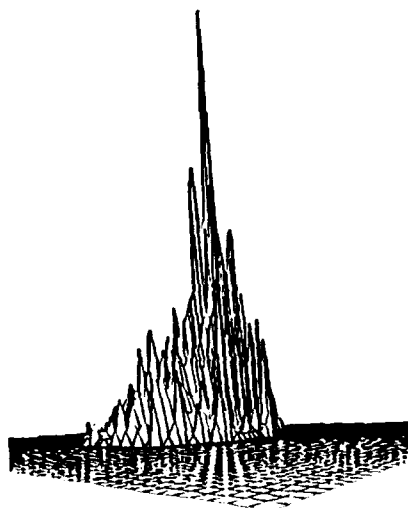
Random colored noise



Helicopter vibration
vertical acceleration



Lorenz equations



Duffing's equation

Figure 4.17 Scaling space joint
probability density functions

V. CONCLUSIONS AND SCOPE FOR FUTURE RESEARCH

Engineering methods of chaos theory were applied to a discrete representation of chaotic systems of equations. The Lorenz equations and Duffing's equation were examined using a time series approach. The time series were generated numerically using a fourth order Runge-Kutta integration scheme. Several simulations were executed varying the equation parameters, the initial conditions, the embedding dimension and the integration step size. Adaptive step size control was not used because it is not compatible with the use of a time embedding procedure to generate a pseudo phase plane. However, time stepsize affected the Fourier spectrums of the systems analyzed. Small step size acted as a low pass filter in the chaotic dynamical systems. For certain parameters, the systems produced Lyapunov exponents and fractal dimension that indicated the presence of chaos. The size of the embedding dimension was found to affect the chaotic nature of the systems. The best embedding dimensions were found to be between one and ten. Large embedding dimensions caused the pseudo phase plane to have a different nature than the phase plane.

A new method, the multivariate scaling analysis, was applied using embedding coordinates to the Lorenz equations and Duffing's equation as well as to the helicopter vibration

data studied by Sarigul-Klijn. A uniformly distributed random time series and a normally distributed random time series were also examined using this new technique. When examined using the multivariate scaling analysis, chaotic systems yielded probability density functions that were nearly Gaussian. The normally distributed random time series produced a density function that was Gaussian in nature. Lastly, the helicopter vibration data yielded a density function that was non-Gaussian, indicating a small amount of chaos in helicopter vibrations.

Many avenues are open to further research in this area. Techniques have been developed that allow accurate prediction of future points in a chaotic time series. This technique can be used to predict the next 5000 points in a time series for helicopter vibrations. This technique could be applied to the currently available data. A higher harmonic control device utilizing this technique could be used to actively dampen the helicopter vibrations. The multivariate scaling analysis could be used to examine other experimental data that appears to have a chaotic nature. This technique offers further evidence of the chaotic nature of the system.

The Naval Air Test Center will soon instrument an H-60 helicopter with a higher harmonic control system. The methods described herein could be applied to the data obtained from that study. This would offer further evidence of the chaotic

nature of helicopter vibrations and help to determine if vibration data can be accurately predicted and hence significantly reduced.

APPENDIX A

PROGRAM TO PERFORM NUMERICAL INTEGRATION

```

*-----
*   This program solves systems of ordinary differential equations
*   using a fourth order Runge-Kutta Scheme.
*
*   The program was used to solve both Duffing's equation and the
*   Lorenz equations.
*
*   Two subroutines are employed.
*       DERIVS calculates the values for the ODE's
*       RK4 is the Runge-Kutta routine
*
*   As written the program does not use an adaptive step-size
*
*   The variables are defined as follows:
*       N - the number of ODE's in the system
*       NMAX - the number of points saved for plotting
*               Currently the program saves every tenth point in a
*               file called RKDAT.DAT
*       H - the desired stepsize
*       X,Y,Z - the independent variables
*               Currently the program solves for only three
*               variables. If a system has more than three
*               equations the additional variables must be
*               declared.
*       F - the ODE's
*               the equations must be specified in the subroutine
*               'DERIVS'
*       Tim - time stored as a vector
*
*   All other variables are working storage spaces
*
*   The current program solves the duffing's equation
*   with parameters:
*       SIG, R, B
*
*   Currently, the output matches the HHC data from Hughes
*
*   The Main Program
*
*   PARAMETER (N=2,NMAX=9990)
*   IMPLICIT DOUBLE PRECISION(A-H,O-Z)
*   CHARACTER*7 DUMMY
*   DATA H,A,B/.1,7.5,0.5/
*   DIMENSION XO(N),XEND(N),F(N),XK1(N),XK2(N),XK3(N),XK4(N),TO(10)
*   COMMON /PARS/H,A,B
*
*   TIME=0.0
*
*   *****
*   *   set the initial conditions
*   *   *****
*
*   DATA XO/0.1,4.1/

```

```

DUM=0.0
DUMMY=' AaaaaA'

OPEN(8,FILE='d1',STATUS='old')

*****
*
*   the lines of text are added to make the data compatible
*   with the program 'CHAOS'
*
*****
WRITE(8,'(A)') ' xxxxxxxxxxxxxxxxxxxxxxxxxxxxxxxxxxxxxxxxxxxxxxxx'
WRITE(8,'(A)') ' xxxxxxxxxxxxxxxxxxxxxxxxxxxxxxxxxxxxxxxxxxxxxxxx'
WRITE(8,'(A)') ' xxxxxxxxxxxxxxxxxxxxxxxxxxxxxxxxxxxxxxxxxxxxxxxx'

DO 11 I=1,NMAX
    X=XO(1)
    Y=XO(2)
    TIME=TIME+H

*****This statement makes the data compatible with 'CHAOS'*****

    WRITE(8,100) DUMMY,TIME,X,Y,X,DUM,DUM

    CALL RK4(XO,XEND,F,N,TIME,XK1,XK2,XK3,XK4)

    DO 14 L=1,N
        XO(L)=XEND(L)
14      CONTINUE

12      CONTINUE

11      CONTINUE
100     FORMAT(A7,F8.3,E11.4,4E12.4)

    STOP
    END

SUBROUTINE RK4(XO,XEND,F,N,TIME,XK1,XK2,XK3,XK4)
*
*   This subroutine performs numerical integration using 4th order
*   Runge-Kutta methods

    IMPLICIT DOUBLE PRECISION(A-H,O-Z)
    COMMON /PARS/H,A,B
    DIMENSION F(N),XO(N),XEND(N),XK1(N),XK2(N),XK3(N),XK4(N)

*   DERIVS returns values for the ODE's
*   Each loop is a step for N equations

    CALL DERIVS(XO,TIME,F,N)
    DO 51 K=1,N
        XK1(K)=H*F(K)
        XO(K)=XO(K)+XK1(K)/2.0D0
51      CONTINUE

    CALL DERIVS(XO,TIME,F,N)

```



```

                XK2(K)=H*F(K)
                XO(K)=XO(K)+XK2(K)/2.0D0
52      CONTINUE

        CALL DERIVS(XO,TIME,F,N)
        DO 53 K=1,N
                XK3(K)=H*F(K)
                XO(K)=XO(K)+XK3(K)
53      CONTINUE

        CALL DERIVS(XO,TIME,F,N)
        DO 54 K=1,N
                XK4(K)=H*F(K)
54      XEND(K)=XEND(K)+(XK1(K)+2.0D0*XK2(K)+2.0D0*XK3(K)+XK4(K))/6.0D0
        continue

        RETURN
        END

```

```

SUBROUTINE DERIVS(XO,T,F,N)

```

```

*      This subroutine obtains values for the ODE's
*      This subroutine must be changed for a new system of equations
*      This routine solves Duffing's equation

```

```

        IMPLICIT DOUBLE PRECISION(A-H,O-Z)
        COMMON /PARS/H,A,B
        DIMENSION F(N),XO(N)
        F(1)=XO(2)
        F(2)=A*COS(T)-XO(1)**3-B*XO(2)

```

```

        RETURN
        END

```

```

*****
*      use this routine to solve the Lorenz equations
*****
*      IMPLICIT DOUBLE PRECISION(A-H,O-Z)
*      COMMON /PARS/SIG,B,R,H
*      DIMENSION F(N),XO(N)

*      F(1)=SIG*(XO(2)-XO(1))
*      F(2)=R*XO(1)-XO(2)-XO(1)*XO(3)
*      F(3)=XO(1)*XO(2)-B*XO(3)
*
*      RETURN
*      END
*****

```

APPENDIX B MULTIVARIATE SCALING ANALYSIS

```
*      This program performs a multivariate scaling analysis
*      on a time series constructed from a numerical integration
*      or generated from experimental results. The program uses the
*      central limit theorem to approximate a standard gaussian
*      distribution so that if the data is truly random the distribution
*      will be random. If the data is chaotic the data will be skewed
*      from the normal distribution.
```

```
*      parameters:
*          ntot      total values in sequence
*          n          values to be plotted. fewer values are plotted
*                   because an imbedding process is used to generate a
*                   sequence.
*          j          the number of divisions on each axis
*          x          the initial data values
*          xs         the standardized values
*          xx         the values on the x-axis for the graph
*          yy         the values on the y-axis for the graph
*          s          sets up the view for the graph
*                   this can be rotated(see grafit manual)
*          amp        the function values for the graph (z-values)
*          work       a workspace grafit uses to generate the graph
```

```
CHARACTER*7 DUMMY
CHARACTER*10 FNAME
real AMP(101,101),COUNT(101),Y(3000),YS(10000),TIM(3000)
real X(3000),XS(10000),XX(101),YY(101),S(6),WORK(24440)
DIMENSION DUMMY(100),A(100),B(100),C(100),D(100)
data S/-8.0,-6.0,3.0,0.0,0.0,0.0/
```

```
WRITE (6,*) 'ENTER THE NUMBER OF DATA POINTS'
READ (5,*) NTOT
```

```
WRITE (6,*) 'ENTER THE EMBEDDING VALUE'
WRITE(6,*) ' This should be an integer value between'
WRITE(6,*) ' 0 and 100'
READ (5,*) NSHIFT
```

```
N=NTOT+NSHIFT
```

```
*      variables:
*          axis      the discrete values on the axes
*          l          the number used for the embedding process
*          xs         the original data values
*          x          the standardized data values
*          y          the embedded data values(standardized)
*          istep      the number of values on each axis
```

```
*****
*
*      read a file here
*
*****
```

```

WRITE(6,*) 'ENTER THE FILENAME'

READ(5,'(A)') FNAME
OPEN(UNIT=8,FILE=FNAME,STATUS='OLD')

DO 10 I=1,N
  READ(8,300) tim(i),x(i)
10  CONTINUE
*****
*
*  As written this format statement must be changed to
*  correspond to the data file to be read
*
*****
300  FORMAT(t8,f6.3,t25,e12.4)

CALL OPNGKS(1,2,1)

*****
*  embedding procedure
*****

DO 11 I=1,NTOT
  Y(I)=X(I+NSHIFT)
11  CONTINUE
*****
*
*  standardize the variables
*
*****

TOTAL=0.0
DO 21 I=1,NTOT
  TOTAL=TOTAL+X(I)
21  CONTINUE

RNTOT=NTOT
XBAR=TOTAL/RNTOT

SUM=0.0
DO 22 I=1,NTOT
  SUM=SUM+((X(I)-XBAR)**2)
22  CONTINUE

XSIGMA=SQRT(SUM/RNTOT)

DO 23 I=1,NTOT
  X(I)=(X(I)-XBAR)/XSIGMA
23  CONTINUE

TOTAL=0.0
DO 31 I=1,NTOT
  TOTAL=TOTAL+Y(I)
31  CONTINUE

```

```

SUM=0.0
DO 32 I=1,NTOT
    SUM=SUM+((Y(I)-YBAR)**2)
32 CONTINUE

YSIGMA=SQRT(SUM/RNTOT)

DO 33 I=1,NTOT
    Y(I)=(Y(I)-YBAR)/YSIGMA
33 CONTINUE

```

```

*****
*   construct a scaling space for variables
*****

```

```

nt=0
do 12 i=1,ntot
    do 13 j=1,ntot
        if(i.eq.j)then
            go to 13
        else
            nt=nt+1
            xs(nt)=x(i)-x(j)
        endif
    continue
13 continue
12 continue

nt=0
do 14 i=1,ntot
    do 15 j=1,ntot
        if(i.eq.j)then
            go to 15
        else
            nt=nt+1
            ys(nt)=y(i)-y(j)
        endif
    continue
15 continue
14 continue

DO 40 I=1,13
    COUNT(I)=0.0
40 CONTINUE
NTO=NTOT**2-NTOT

```

```

*****
*
*   This section of the program calculates the 'z' coordinate
*   for the PDF. The 'xmin' and 'xmax' values are the beginning
*   and end points for each grid in the x-y plane. ( Similarly
*   for 'ymin' and 'ymax' )
*
*
DO 60 I=1,101
    DO 61 J=1,101

```

```

60      CONTINUE

      DO 50 I=1, NTO
      XMIN=-5.0
      XMAX=-4.9

          DO 51 K=1, 101
          IF (XS(I).GE.XMIN.AND.XS(I).LT.XMAX) THEN
              IXC=K
              GO TO 52
          ELSE
              XMIN=XMIN+.1
              XMAX=XMAX+.1
          ENDIF
51      CONTINUE
52      YMAX=-5.0
      YMIN=-4.9

          DO 53 K=1, 101
          IF (YS(I).GE.XMIN.AND.YS(I).LT.YMAX) THEN
              IYC=K
              GO TO 54
          ELSE
              YMIN=YMIN+.1
              YMAX=YMAX+.1
          ENDIF
53      CONTINUE
54      AMP(IXC,IYC)=AMP(IXC,IYC)+1
50      CONTINUE

      DO 66 I=1, 101
      XX(I)=I
      YY(I)=I
66      CONTINUE

      CALL SRFACE(AMP,101,101,101,XX,YY,WORK,S,0.0)

      CALL CLSGKS

      STOP
      END

```

LIST OF REFERENCES

- 1.1 National Research Council, "David II Report," *Notices of the American Mathematical Society*, pp.813-837, November 1990.
- 1.2 Sarigul-Klijn, M., "Application of Chaos Methods to Helicopter Vibration Reduction Using Higher Harmonic Control," Ph.D. Dissertation, Naval Postgraduate School, Monterey, CA March 1990.
- 1.3 Osborne, A., and Provenzale, A., "Finite Correlation Dimension for Stochastic Systems with Power Law Spectra," *Physica D*, V.35, pp.357-381, 1989.
- 2.1 Devaney, R., *An Introduction to Chaotic Dynamical Systems*, 2nd ED., Addison Welsey, 1989.
- 2.2 Sandefur, J., *Discrete Dynamical Systems*, Clarendon Press, 1990.
- 2.3 Barnsley, M., *Fractals Everywhere*, Harcourt Brace Jovanich, 1988.
- 2.4 Bloomfield, P., *Fourier Analysis of Time Series*, John Wiley and Sons, 1976.
- 2.5 Takens, F., "Detecting Strange Attractors in Turbulence," *Lecture Notes in Mathematics*, Springer Verlag, V.898, 1981.
- 2.6 Moon, F., *Chaotic Vibrations*, John Wiley and Sons, New York, 1987.
- 2.7 Grassberger, P., "Estimating the Fractal Dimension and Entropies of Strange Attractors," *Chaos*, pp.291-311 Princeton University Press, 1986.
- 2.8 Dvorak, I., and Klaschka, J., "Modification of the Grassberger-Procaccia Algorithm for Estimating the Correlation Exponent of Chaotic Systems with High Embedding Dimension," *Physics Letters A*, V.145, No.5, pp.225-231, 16 April 1990.
- 2.9 Hammel, S., "A Noise Reduction Method for Chaotic Systems," *Physics Letters A*, V. 148, No.8, pp.421-428, 3 September 1990.

- 2.10 Guckenheimer, J., and Holmes, P., *Nonlinear Oscillations, Dynamical Systems and Bifurcations of Vector Fields*, Springer-Verlag, 1983.
- 2.11 Thompson, J., and Stewart, H., *Nonlinear Dynamics and Chaos*, John Wiley and Sons, 1986.
- 2.12 Wolf, A., Swift, J., Swinney, H., and Vastano, J., "Determining Lyapunov Exponents from a Time Series," *Physica D*, V.16, pp.285-317, 1985.
- 2.13 Kapitaniak, T., and Naschie, J., "A Note on Randomness and Strange Behavior," *Physics Letters A*, V. 154, No.6, pp. 249-253, 8 Apr 91.
- 2.14 Ruelle, D., "Deterministic Chaos: The Science and the Fiction," Lecture delivered in London, *Proceedings of the Royal Society of London*, V. A427, 23 October 1989.
- 2.15 Farmer, J., Ott, E., Yorke, J., "The Dimension of Chaotic Attractors," *Physica D*, V.7, pp.153-180, 1983.
- 2.16 Lindsay, P., "An Efficient Method of Forecasting Time Series Using Linear Interpolation," *Physics Letters A*, V 153, No. 6, pp. 353-356, 11 Mar 91.
- 2.17 Bleher, S., Grebogi, C., and Ott, E., "Bifurcation to Chaotic Scattering," *Physica D*. V. 46, No. 1, pp. 87-121, Oct 90.
- 2.18 Hughes, D., and Proctor, M., "Chaos and the Effect of Noise in a Model Three-wave mode Coupling," *Physica D*. V. 46, No.2, pp. 163-176, Nov 1990.
- 2.19 Corless, R., Frank, G. and Monroe, J., "Chaos and Continued Fractions," *Physica D*, V. 46, No.2, Nov. 1990.
- 2.20 Higuchi, T., "Relationship Between the Fractal Dimension and the Power Law Index for a Time Series: A Numerical Investigation," *Physica D*, V. 46, No. 2, Nov. 1990.
- 2.21 Liebert, W., and Schuster H., "Proper Choice of the Time Delay for the Analysis of a Chaotic Time Series," *Physics Letters A*, V.142, No. 2, pp. 107-111, 4 Dec 89.
- 2.22 Fang, J., "The Effects of White Noise on Complexity in a Two Dimensional Driven Damped Dynamical System,"

Physics Letters A, V. 142, No. 6., pp. 344-348, 18 Dec 89.

- 2.23 Kapitaniak, T., "Analytical Condition for the Chaotic Behavior of the Duffing Oscillator," *Physics Letters A*, V. 144, No. 6, pp. 322-324, 12 Mar 90.
- 2.24 Chen, Q., and Ott, E., "Cross Sections of Strange Attractors," *Physics Letters A*, V. 147, No. 8, pp. 450-454, 30 Jul 90.
- 2.25 Stone, E., "Power Spectra of the Stochastically Forced Duffing Oscillator," *Physics Letters A*, V. 148, No. 8, pp.434-442, 3 Sep 90.
- 3.1 Ueda, Y., "Steady Motions Exhibited by Duffing's Equation," *New Approaches in Nonlinear Dynamics*, Ed. Holmes,P., pp. 422-434, 1980.
- 3.2 Gerald, F. and Wheatley, P., *Applied Numerical Analysis*, 4th. Ed., Addison Wesley, 1989.
- 3.3 Press, Flannery, Teukolsky and Vetterling, *Numerical Recipes: The Art of Scientific Computing*, Cambridge University Press, 1986.
- 3.4 Nyhoff, L., and Leestma, S., *Fortran 77 for Scientists and Engineers*, 2nd Ed., Macmillan Publishing Company, 1988.
- 4.1 Grassberger, P.,and Procaccia, I., "Characterization of a Strange Attractor," *Physical Review Letters*, V. 50, pp. 346-349, 31 Jan 83.
- 4.2 Moon, F., and Li, G., "The Fractal Dimension of a Two Well Potential Strange Attractor," *Physica D*, V.17, pp.99-108, August 1985.

INITIAL DISTRIBUTION LIST

- | | | |
|----|--|---|
| 1. | Defense Technical Information Center
ATTN: Selection Section (DTIC-FDAC)
Building 5
Cameron Station
Alexandria, VA 22304-6145 | 2 |
| 2. | Library, Code 0142
Naval Postgraduate School
Monterey, CA 93943-5002 | 2 |
| 3. | Department Chairman, Code 67
Department of Aeronautics and Astronautics
Naval Postgraduate School
Monterey, CA 93943-5000 | 1 |
| 4. | Department of Aeronautics and Astronautics
ATTN: Professor Ramesh Kolar, Code AA/Kj
Naval Postgraduate School
Monterey, CA 93943-5000 | 7 |
| 5. | Commander
Naval Aviation Depot
Code 0412
ATTN: CDR Sarigul-Klijn
Alameda, CA 94501-0000 | 1 |
| 6. | Captain Edward A. Healy, Jr.
587-A Connor Road
West Point, NY 10996-0000 | 2 |